NAZARBAYEV UNIVERSITY

Bachelor of Engineering
(Mechanical)

# DESIGN OF A BUS SHELTER BASED ON GREEN ENERGY TECHNOLOGIES FOR EXTREME WEATHER CONDITIONS IN ASTANA

Report on Capstone Project II

By

Alikhanova Arailym

Kakimzhan Aldiyar

Mukhanov Anuarbek

Principal Supervisor: Luis R. Rojas-Solórzano

April 2017

## DECLARATION

We hereby declare that this report entitled "*Design of a bus shelter based on green energy technologies for extreme weather conditions in Astana"* is the result of our own project work except for quotations and citations, which have been duly acknowledged. We also declare that it has not been previously or concurrently submitted for any other degree at Nazarbayev University.

- - - - - - - - - - - - - - - - - - - - - - - - - - - - - - - - - - - - - - - - - - - - - - -

Name: Alikhanova Arailym

Date:

- - - - - - - - - - - - - - - - - - - - - - - - - - - - - - - - - - - - - - - - - - - - - - -

Name: Kakimzhan Aldiyar

Date:

- - - - - - - - - - - - - - - - - - - - - - - - - - - - - - - - - - - - - - - - - - - - - - -

Name: Mukhanov Anuarbek

Date:

## Acknowledgements

We owe special gratitude to Professor Luis R. Rojas-Solórzano for supervising and encouraging us throughout the work on the Capstone Project. We also want to thank School of Engineering at Nazarbayev University, especially Professor Jong Kim for helping us to gather information about soil layers in Astana and Professor Konstantinos Kostas for competent organization of the Capstone Project course. Finally, we would like to express deepest and sincere gratitude to our parents for their love, inspiration and support.

## Abstract

Nowadays the contribution of renewable energy sources to the worldwide energy demand is already significant and the trend is expected to be accentuated. The reasons are the numerous benefits such as reduction in greenhouse gas emission and dependence on fossil fuels. The Republic of Kazakhstan is also concerned with the development of the renewable energy sector. Moreover, green energy technologies in combination with conventional technologies can result in more economic solutions for various applications. The transportation segment has recently experienced rapid development in Astana and one of the popular projects in the city is the construction of "warm" bus shelters. Nevertheless, there are several problems with current bus shelters such as insufficient space for passengers and the high costs of existing technologies. Thus, this project proposes the modernization of the shelter at "Cardiac Surgery Center" bus stop by using an optimal combination of clean and conventional energy sources. Three types of green energy technologies: ground source heat pumps, solar panels and wind turbines, are assessed for technical and financial viability. Thermal heating loads, originally served by electric heaters, are planned to be served in our proposal by combined geothermal and conventional electric heater system, whereas wind turbines and solar panels are intended to partly feed electric load.

The technical and financial viability analyses were performed using RETScreen 4 and HOMER LEGACY state-of-the-art software platforms, which permit to model complex energetic systems and determine the technical viability, while evaluating the cash flow life cycle cost performance within given financial and market conditions. Once our source-technology-demand-supply energy model was created, the simulations demonstrated that including a geothermal heat pump unit to the system would be a profitable solution with relatively short payback period. However, possible combinations of grid electricity with wind and solar energy technologies resulted in higher net present cost than the conventional only-grid connected system.

Proper design of a geothermal heat pump unit requires accurate evaluation of thermal properties of underground soil layers and their temperature distribution. For the city of Astana the results show that the most suitable design is a horizontal geothermal system with 70m-long tubes buried at 10m depth. The total initial cost of the project is 11520 USD. In addition, the proposed green energy technology saves around 6159 USD in 25 years due to efficient electrical energy consumption. More importantly, application of the geothermal heat pump unit reduces GHG emission by 2.8 $tCO_2$ annually. Lastly, the suggested shelter cabin design is twice larger in size than original and can accommodate up to 50 passengers. Therefore, it can be concluded that the proposed bus shelter design is more efficient, environmentally friendly, spacious and economically attractive.

## Table of contents

**List of Figures**

**List of Tables**

## List of Abbreviations, Notations / Glossary of Terms

COP – coefficient of performance

GHG – greenhouse gases

GSHP – Ground Source Heat Pump

NPC – Net Present Cost

NPV – Net Present Value

PV panels – photovoltaic panels

IRR – internal rate of return

## 1. Introduction

Renewable energy sources such as solar, wind, marine, hydropower, geothermal, and biomass, have recently gained a lot of attention as alternatives for electricity generation. Overall, they contribute to 15-20% of the worldwide energy demand. This figure is expected to increase to 30% by 2020 and to 50% in 2050 (Mohammed et al., 2016). Likewise, Republic of Kazakhstan is also concerned with the development of the renewable energy sector. This is evident from the main theme of EXPO-2017 ASTANA, which is development of "green energy" (EXPO-2017 ASTANA, 2016). In addition, transportation sector has been one of the fastest developing segments in Astana since the establishment of "Astana Transportation Authority" in 2011.

One of the popular projects in this sector is the construction of "warm" bus shelters. However, there are still several problems like the lack of space in the bus shelter for passengers and the high cost of the existing technologies. In addition, transition to renewable energy sources would be a logical next step within the framework of EXPO-2017. Therefore, our project proposes modernization of the bus shelter at "Cardiac Surgery Center" bus stop (in front of "Asia Park" shopping mall) with clean energy sources, particularly solar and wind for electricity supply, and geothermal unit for heat generation. This will be achieved through the simulation of multiple technologies and financial scenarios to determine the best suiting hybrid clean energy system.

Our goal is to perform feasibility analysis of our proposed systems, i.e. find the best combination of the conventional grid, solar panels, wind turbines, and a geothermal unit. These hybrid systems will be properly dimensioned and afterwards, compared economically against the conventional systems in terms of their net present costs. The system with the lowest NPC will be chosen for construction. Another objective to be achieved is to expand the overall area of the bus shelter in order to accommodate most of the passengers needing that service during a regular day. After the most cost-effective system is determined, a

detailed design of the new bus shelter will be performed, so that it can be readily implemented at the site.

The project is divided into several parts. Firstly, the site chosen, i.e. “Cardiac Surgery Center” bus stop will be evaluated for sufficiency of solar and wind energy sources. Secondly, a field survey will follow by counting the number of passengers at the bus stop in a typical day. Then, a new size of the bus shelter will be calculated accordingly. After that, based on the results of the field experiment and on heat transfer equations, the overall heat loss of the bus shelter will be calculated throughout the year. Next, a RETScreen model will be constructed and life cycle cost simulations of heating demand-supply will be performed in order to compare geothermal technology combined with electric heaters with the existing fully electric heating base case. The final step is to calculate the electric load of the bus shelter and create an energy system model using HOMER LEGACY platform to simulate and find the best combination of solar, wind and conventional (electric grid) technologies. In addition, the selected design will be further developed in terms of its technical characteristics. Finally, thorough economic analysis, installation and maintenance schedules, and the total cost of the proposed design are also presented in the framework of this project.

## 2. Literature review and background material

### 2.1. Existing technology

Current bus stops and bus traffic are regulated by LLP "Astana Transportation Authority" (ASTRA, 2016). It was established in 2011 for implementation of innovative projects in the transport industry with application of new technologies. One of the projects implemented since then is building of new "warm" bus shelters. The purpose of this innovation is to provide public transport passengers with comfortable conditions and protection from severe weather as snow, rain and frost. There are already 27 bus shelters constructed in Astana, and it is planned to build 55 more in the following year (ibid).

The existing bus shelter "Cardiac Surgery Center" is located at the intersection of Kabanbay batyr avenue and Dostyk street. This site was chosen by "ASTRA" to be the first one for building a new "warm" bus shelter in 2015. There were several important reasons for this decision. Firstly, it is one of the busiest bus stops in the city. Secondly, it is a transport hub, i.e. a transfer point with a large number of urban, suburban and express routes passing through (ibid). For the exact same reasons, we chose this place for modernization with clean energy technologies.

The current bus shelter utilizes conventional electrical grid system to supply all its heating and power demand. The heating is provided by electrical radiant heaters. Some of the extra features include information screens and a video surveillance system (ibid). However, one of the main drawbacks of the current design is lack of sheltered space. They cannot accommodate most of the people waiting for the buses. Our aim was to design a bus "station" with sufficient space for most of the waiting passengers and reduce grid electricity usage by utilizing clean energy technologies in an economic and eco-friendly manner.

## 2.2. Renewable sources of energy

It is a known fact that power networks using conventional energy come up with high level of fossil fuel consumption and environmental costs due to greenhouse gas emissions (Huang et al., 2011). Therefore, a huge amount of research has been devoted to developing sustainable energy systems, which would be considered as both cost-effective and environment-friendly at the same time. In order to achieve this goal, renewable sources of energy (utilizing local natural resources and networks) are considered to be the best solution (Erdinc and Uzunoglu, 2012). However, Erdinc and Uzunoglu (2012) also point out, that even though each of these renewable sources has a number of advantages over conventional sources of energy, one disadvantage of them is their unpredictable nature and weather/climatic conditions dependence. Therefore, hybrid energy systems were successfully introduced and are getting increasing attention of researchers, with fossil fuel usage as emergency backup only (Huang et al., 2011). Figure 2.1 illustrates the general architecture of a hybrid system.

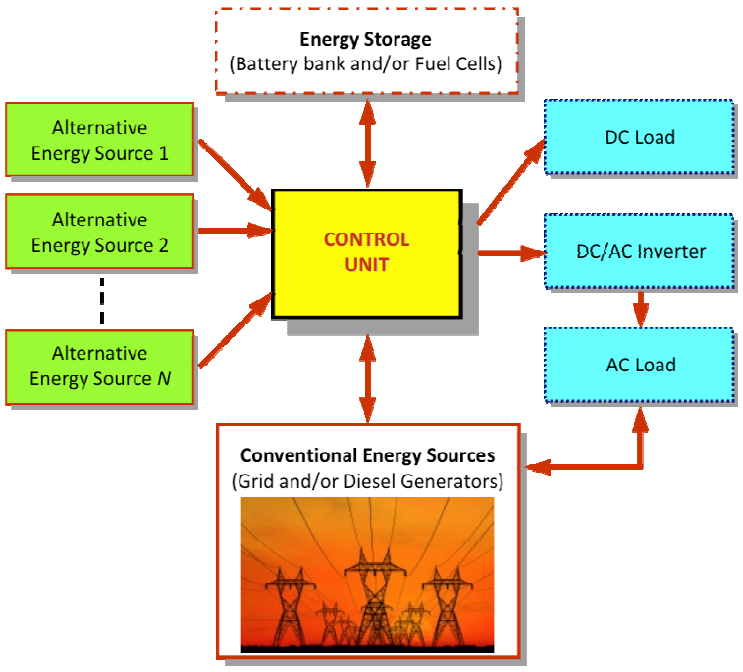


Figure 2.1. General architecture of a hybrid system (adapted from Mohammed et al., 2016)

Renewable sources of energy considered in the project are solar, wind and geothermal.

### 2.2.1. Solar Power

The Earth receives about 174 million gigawatts (GW) of solar radiation at the level of upper atmosphere. More than a half of this energy is either reflected back or absorbed by the atmosphere and oceans (Smil, 1991). According to a study by United Nations Development Programme and World Energy Council in 2000, it was estimated that the global solar energy has a potential of generating from 1575 to 49837 exajoules (EJ) of energy annually. This number is several times higher than the current annual worldwide energy consumption of 559.8 EJ (IEA, 2014). Therefore, solar energy has a great potential and should certainly be harvested and researched further. The total energy generated by PV systems worldwide is now 200 TWh, which contributes to 1% of overall electricity demand (Solar Power Europe, 2012). The production of PV panels increases by more than 100% each year, while the cost of solar panels is declining (PVinsights, 2011). The original price of solar cells in 1970 was 150$/W, which since then has decreased to 0.6$/W. It is estimated that by the year 2030, 9% of worldwide electricity consumption could be generated by PV systems, while by 2050 this figure can increase to 20% (EPIA, 2012).

### 2.2.2. Wind Power

Wind power generation has been significantly developing in recent years. The wind electricity generation worldwide is increasing exponentially and the overall trend can be observed in Figure 2.2 (WWEA, 2014).

The wind-generated energy constitutes 4% of electricity demand over the world (WWEA, 2014) and 11.4% in Europe. Moreover, wind energy is becoming more favorable than conventional energy sources. For instance, 44% of new installed capacity in 2015 was in form of wind power, while the fossil fuel capacity decreased (EWEA, 2015).

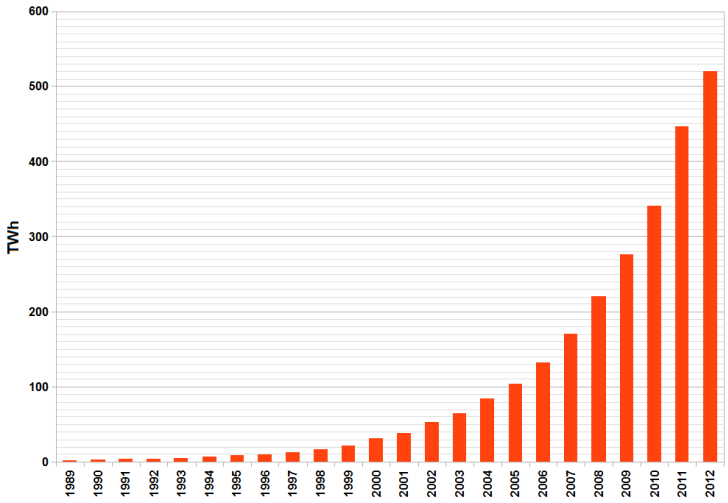


Figure 2.2. Worldwide electricity generation from wind (WWEA, 2014)

Kazakhstan, in particular, has a great potential of wind power generation. About 50% of its territory has average wind speeds of 4-5m/s at a height of 30m and the overall wind energy generation potential of the country is 1820 GWh per year. The sites with the largest potential are located in Caspian Sea, Karaganda and Akmola regions (see Figure 2.3). Therefore, Kazakhstan, and especially Astana, are very attractive in terms of wind power generation (UNDP, 2006).

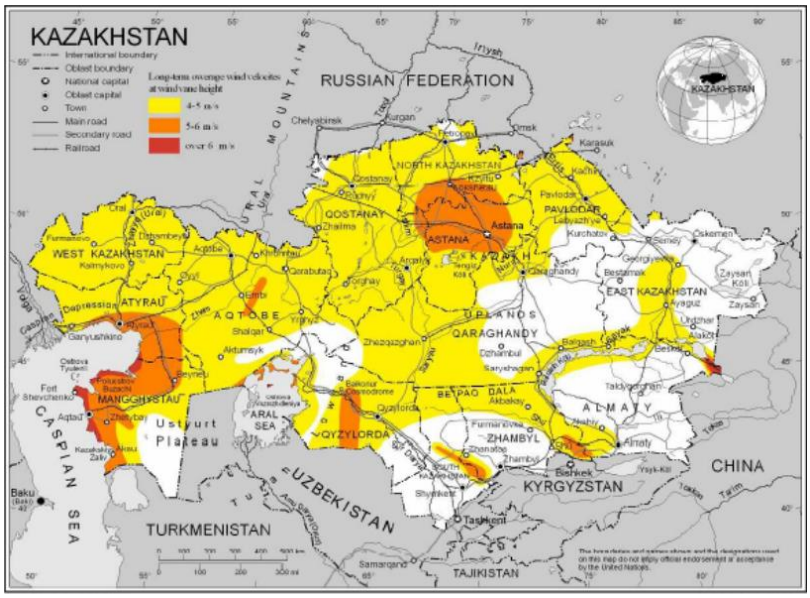


Figure 2.3. Wind Atlas of Kazakhstan (UNDP, 2006)

### 2.2.3. Ground Source Heat pumps (Geothermal unit)

The technology of heat pump application to a ground energy source is in practice for more than 50 years. Even though before 1970's the use of subsurface energy was not very trendy in industry, it gained more popularity as the oil scarce problem arose (Pennsylvania Clean Stream Law, 2001).

What is earth energy? Earth obtains heat from the sun, then provided heat is conducted into the ground, after which the earth uses few meters of surface soil layers as insulation to keep itself warm and act like a renewable source of energy (Rawlings et al., 2004). This results in a relatively constant underground temperature regardless of seasonal temperature changes on the surface. The earth temperature a number of meters below the surface of the ground is constantly cooler than the air temperature during the summer and warmer during winter period of time (US Department of Energy, 2011). To be more precise, from 1.5 to 15 meters below the surface, the earth temperature remains almost constant, and increases by only 1ºC with each 30 m in depth (Pennsylvania Clean Stream Law, 2001). Since the variations in underground temperature are almost negligible, the geothermal heat pumps are provided as wintertime heat sources and summertime heat sinks (US Department of Energy, 2011).

Mainly, geothermal heat pumps consist of three main component, namely ground loop, heat pump and distribution loop (European Geothermal Energy Council, 2009). Ground loop is a pipeline filled with antifreeze solution that passes through the underground transferring energy to a heat pump, which in turn extracts this energy with the aid of a secondary fluid. Finally, the heated fluid goes through a distribution loop with a fan in a conditioned space (Meyer et al., 2011). Table A.1 in Appendix A gives more detailed description of each sub-system with own components and their functions.

There are a number of common configurations for transfer of energy, classified into two groups, namely open loop or closed loop transportation systems (Canadian GeoExchange Coalition, 2009). Closed loop systems include types such as horizontal, vertical and pond/lake. In order to make the best choice in a given application, a number of factors like climate, soil conditions, availability of land and water resources need to be considered (US Department of Energy, 2011).

*Open loop systems* use underground water or surface body water as a circulation fluid to transfer energy. Therefore, this choice is appropriate in case of enough supply of clean underground water (ibid). Moreover, this has a number of disadvantages regarding fouling and corrosion. Therefore, closed loop systems are more popular in application.

*Closed loop systems* may be of *horizontal*, *vertical* or *pond type*. Closed-loop systems operate based on the circulation of the antifreeze solution across underground loop pipes, which act like underground heat exchanger, transporting the energy (Pennsylvania Clean Stream Law, 2001). Horizontal loops are considered to be best in terms of cost-effectiveness, but only if land area is sufficient (US department of energy, 2011). These loops are placed in narrow, 1.5-3 m deep trenches that are tens of meters long.

*Vertical closed loop systems* are installed in drilled borings. Typically, 38-61 meters of borehole is required per ton of heating/cooling unit (ibid). They are applied where land area is limited, or when the soil is too shallow to bury. Vertical loops run perpendicular to the surface and the holes can be several hundred feet deep. At these depths, the undisturbed ground temperature does not change throughout the year.

*Pond/lake systems* may require least expenses if the field has enough amount of water body (ibid). Figure 2.4 illustrates the different ground loop configurations.

The most viable hybrid combination of these above explained three renewable sources needs to be determined. Simulation programs are the most common tools for assessing performance of these hybrid systems. With the aid of them, the optimum configurations can be found. One of such simulation tools is HOMER developed by National Renewable Energy Laboratory (NREL), in the USA (Erdinc and Uzunoglu, 2012).

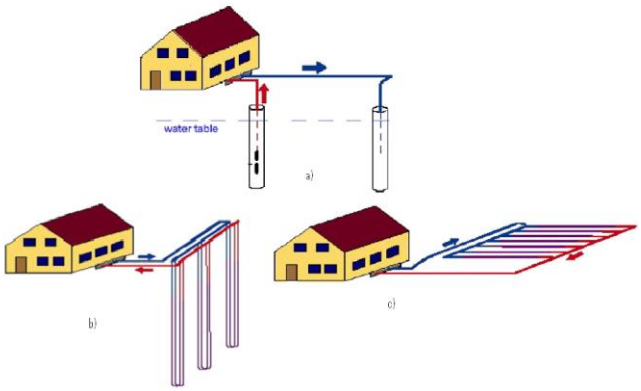


Figure 2.4. Ground-loop configurations: a)open-loop borehole, b)closed-loop vertical, c)closed-loop horizontal (adapted from Meyer et al., 2011).

## 2.3. Homer Software

HOMER is a simulation platform, which, allows the user to create time-based energy demand-supply models, providing a set up to perform life-cycle cost analyses under specified financial and economic conditions. It mainly simulates the operation of a hybrid micro-grid for a whole year, in time steps from one minute to one hour. For each minute or hour HOMER compares the input loads and makes calculations for each system configuration to supply the demand. In order to rightly design a system, a number of decisions on configuration of the system must be made, related to type and size of each component. Then, our HOMER model will consider these as inputs to simulate different combinations, and will give results in table-format prioritizing the systems according to Net Present Cost.

### 2.4. RETScreen Software

RETScreen is a Clean Energy Management Software package developed by the Government of Canada for energy efficiency, performance and cogeneration project viability analysis (Natural Resources, 2016). The package includes a free excel-based decision support tool called RETscreen 4. The tool is developed by team of industry, government and academia experts from CanmetENERGY research center (RETScreen, 2015). It aids to identify, assess and optimize the technical and financial viability of potential clean energy project. In the project, RETScreen will allow us to build a yearly-based energy model and use it to compare the system with Ground Source Heat Pump and electric heaters vs the system with entire demand served by electric heaters. Our RETScreen model estimates the NPV and Payback Period for each combination in order to choose the system maximum of savings.

Our proposed renewable energy hybrid system will consist of solar panels and wind turbine to generate electricity consumed by the shelter, while Ground Source Heat Pump in will be operating to supply the shelter with heat only.

## 3. Methods and Tools description

### 3.1. Site evaluation

#### 3.1.1. Sun irradiation simulation

The next step is to estimate if the amount of sun irradiation and wind resources is sufficient to install these types of renewable energy systems. For this purpose, 3D models of the bus station and surrounding buildings were developed in SketchUp software. The layout of the CAD model can be seen in Figures C.1 and C.2 in Appendix C.

The first simulation was carried out in Shadow Analysis plug-in of SketchUp. This plug-in analyzes surfaces and calculates how many hours during a day the given space is under a shadow. Therefore, the dates with the shortest and longest daylight hours were chosen, i.e. December 21 and June 21. The results of this simulation can be seen in Figures C.3 and C.4 in Appendix C. As it can be seen, on December 21, approximately 1 hour during the daytime the top of the bus shelter is under shadow, whereas on June 21 the duration is about 3 hours. By subtracting this time from the length of the day we calculated a total of 6 hours and 53 minutes of sunlight on December 21, and 13 hours and 34 minutes on June 21 (Time and Date, 2016). Therefore, we can safely assume that we can have from 6 to 13 hours of sunlight during the year, which is more than enough for a solar power system.

### 3.1.2. Wind simulation

The wind simulation, was performed on CFD software PHOENICS-VR. For this purpose the CAD model of bus shelter area and wind data obtained from "Astana Wind Farm: Pre-feasibility study" (UNDP Kazakhstan, 2009) were imported into the software. The wind direction was set to Southwest, as it is the predominant wind direction in Astana. Sample results for January can be seen in Figures C.5-C.7 in Appendix C. The summary of simulation results can be observed in Table 3.1.

Table 3.1. PHOENICS-VR simulation results over the year

| Month | Wind speed at 3m (m/s) | Wind speed at 10m (m/s) | Wind speed at 20m (m/s) | Wind speed at 30m (m/s) |
|---|---|---|---|---|
| January | 7.83 | 8.56 | 9.3 | 10.04 |
| February | 6.29 | 6.88 | 7.48 | 8.08 |
| March | 5.66 | 6.2 | 6.74 | 6.74 |
| April | 5.35 | 5.86 | 6.38 | 6.38 |
| May | 6.45 | 7.06 | 7.67 | 8.27 |
| June | 4.9 | 5.36 | 5.83 | 5.83 |
| July | 4.12 | 4.5 | 4.9 | 4.9 |
| August | 4.04 | 4.42 | 4.81 | 4.81 |
| September | 4.28 | 4.68 | 5.09 | 5.09 |
| October | 4.35 | 4.77 | 5.18 | 5.18 |
| November | 4.98 | 5.45 | 5.92 | 5.92 |
| December | 7.6 | 8.32 | 9.03 | 9.75 |

As it can be seen from Table 3.1, the wind velocity above the site varies between 4m/s and 10m/s, which is sufficient for most of commercially available wind turbines (UNDP, 2006). Therefore, it can be concluded that the site at the bus stop "Cardiac Surgery Center" is able to provide sufficient amount of sunlight and wind energy for operation of solar panels and wind turbines.

### 3.2. Passenger load survey

A field survey was carried out in order to determine the maximum number of people at the bus stop. With the purpose of getting the results as realistic as possible, the number of people was counted several times throughout the day during the several working days.

From the schedule of the bus arrivals, it can be known that buses travel starting from 6 am early morning to 12 am transporting people during 18 hours each day. This time-period was subdivided into 9 sub-periods, each constituting 2 hours.

During the very first day, the bus stop was visited several times with interval of 2 hours in order to determine the most crowded periods. It was found that during three intervals of time, namely 6 am - 8 am, 12 pm – 2 pm and 6 pm – 8 pm, the density of users at bus stop were the highest. Between these crowded time-periods, the number of users were quite small, and close to each other. Therefore, for the rest of days, the intervals between these most crowded periods were merged, leaving us with only 6 time intervals.

During first five working days from Monday to Friday, the bus stop density was checked and numbers were recorded to calculate the average. During the second week, randomly Tuesday, Thursday and Friday were chosen to double-check the results, and since the difference constituted for less than 10% in comparison to first week figures, the experiment was justified.

During each visit to bus stop, the number of people was counted each time the bus arrived, and the average was calculated for the whole period. Each counting period started when the most infrequent bus (bus No 32) arrived, and ended with the arrival of second bus with No 32. Table 3.2 gives the field survey collected and processed data.

The volume of the current bus shelter installed in front of Asia Park by Astana LRT is intended to fit only 35 pedestrians, with dimensions of 5.27x3x3 $m^3$ (alrt.kz). However, as it can be seen from the field data, the maximum average that occurs during the time-period from 6pm to 8pm is 50. Therefore, the net area of the closed bus shelter is decided to be increased to fit 50 people.

Table 3.2. Results of field survey at bus stop

| | Average number of people per period by day | | | | | | | | |
|---|---|---|---|---|---|---|---|---|---|
| | 6 am - 8 am | 8 am - 10 am | 10 am - 12 pm | 12 pm - 2 pm | 2 pm - 4 pm | 4 pm - 6 pm | 6 pm - 8 pm | 8 pm - 10 pm | 10 pm - 12 am |
| Day 1: Monday | 36 | 8 | 10 | 23 | 17 | 15 | 49 | 11 | 9 |
| Day 2: Tuesday | 35 | 11 | | 28 | 12 | | 61 | 9 | |
| Day 3: Wednesday | 30 | 7 | | 34 | 16 | | 52 | 8 | |
| Day 4: Thursday | 42 | 12 | | 18 | 18 | | 47 | 13 | |
| Day 5: Friday | 37 | 9 | | 22 | 9 | | 41 | 8 | |
| ***Average values per period considering 5 day results*** | ***36*** | ***10*** | | ***25*** | ***15*** | | ***50*** | ***12*** | |
| Day 6: Tuesday | 39 | 9 | | 23 | 17 | | 41 | 14 | |
| Day 7: Thursday | 35 | 6 | | 25 | 12 | | 57 | 8 | |
| Day 8: Friday | 43 | 12 | | 21 | 13 | | 43 | 11 | |
| | ***39*** | ***9*** | | ***23*** | ***14*** | | ***47*** | ***11*** | |
| ***Difference in %*** | ***7.70%*** | ***10.00%*** | | ***8.00%*** | ***6.67%*** | | ***6.00%*** | ***8.33%*** | |

### 3.2.1. Sizing of shelter

Based on experiment, calculated average value of people that should be fitted in the new bus shelter design is 50. According to Transit Capacity and Quality of Service Manual, average pedestrian area of Service level D could be 0.5 $m^2$, which is appropriate amount of space per person standing there for not a long period of time. Therefore, total required area for average of 50 pedestrians is calculated to be *25 square meters.* The height and width of the bigger shelter will be held at typical value of *3 meters* both, as also was chosen by Astana LRT company (alrt.kz). Consequently, the length of the station is planned to be *8.3 meters,* to give enough area of 25 $m^2$ as required for 50 people in there. Here, only the length is decided to be prolonged, not width, since with increase in width the access to the doors will get harder and window vision for seeing the bus numbers get less possible.

## 3.3. Heat load calculation

Heat load indicates the amount of energy that must be provided by ground source heat pump to assure the desired comfort level of temperature within a space. Therefore, the accurate sizing of the equipment essentially depends on the heat load amount calculation, so to avoid under- or over- dimensioning of the system. Rightly calculated heating load will dictate the selection of heat pump and heat exchangers length (Burdick, 2011).

The heat load amount depends on heat loss of the space. According to Bhatia (nd), heat loss occurs due to conductive and convective heat transfers:

1) Conductive heat losses through building's walls, floor, ceiling and window glass.
2) Convective losses due to infiltration losses, particularly for heating amount of outdoor air coming from ventilation (ibid).

### 3.3.1. Conductive Heat Loss Calculation

In order to know our conductive heat load, one of the first things to do was to calculate the heat loss from the shelter. Therefore, several important preliminary assumptions were made:

1. Windows will cover the entire front wall, the right wall, and half of the back wall
2. For preliminary study purposes 4k-8-4k windows, which means it has two 4mm glass layers separated by 8mm layer of air, were chosen
3. The remaining sides of the walls, i.e. the left and half of the back wall, and the ceiling will be considered to be made of insulation material ISOVER CARCASS-P37
4. The inside temperature was chosen to be 20°C

To calculate the heat loss from the bus shelter the following heat transfer equations were utilized:

$$Q_{cond} = \frac{k \cdot A \cdot (T_i - T_o)}{t} \quad (3.1)$$

$$Q_{cond} = \frac{A \cdot (T_i - T_o)}{U} \quad (3.2)$$

where

$Q_{cond}$: the rate of heat loss in W;

k: heat conductivity of the material in $\frac{\mathrm{W}}{\mathrm{m}\cdot^{\circ}\mathrm{C}}$;

A: area of the wall in $m^2$;

$T_i$: inside temperature in °C;

$T_o$: outside temperature in °C;

t: thickness of the insulation in m;

U: heat resistivity of windows in $\frac{\mathrm{m}^2\cdot^{\circ}\mathrm{C}}{\mathrm{W}}$.

It is important to remember that the conductivity heat load will be varying in accordance with outside temperature value. Therefore, the monthly approximations are made based on outside average value of temperature for each month. The data is taken from observations of Akmola (Tselinograd) weather station, 7.0 km away from Astana, and is given in Table 3.3.

Heat resistivity of windows is a special value assigned to each type of window, which represents the heat transfer through conduction, convection, and radiation combined. This and other coefficients used in the calculation can be found in Table 3.3.

Table3.3. Constants used in the calculation of heat loss

| | | |
|---|---|---|
| Inside temperature | 20 | C |
| U-value of windows (4k-8-4k) | 0.469 | (m^2*C/W) |
| Heat conductivity of the insulation layer | 0.036 | W/(m*K) |
| Thickness of insulation layer | 0.05 | m |
| Area of the windows | 46.35 | m^2 |
| Area of the walls | 21.45 | m^2 |
| Area of the ceiling | 24.9 | m^2 |

The final values of the heat loss from the windows, walls, and the ceiling can be found in the Table 3.4.

### 3.3.2. Convective heat load calculation

Convective heat loss occurs due to ventilation system, which infiltrates certain amount of air, which additionally needs to be heated. In general, occupants in the closed space have two main requirements in terms of air within the space. First one is to have no impact on health from air breathed in, and the second is that outdoor air must always been blown in into the space, and the old air blown out so to maintain the air circulation and keep the air fresh (Bienfait et al., 1992).

Table 3.4. Heat loss values for each month

| Month | Outside Temperature (C) | Heat Loss from Windows (W) | Heat Loss from Walls and Ceiling (W) | Total Heat Loss (W) |
|---|---|---|---|---|
| January | -15.8 | 3538.0 | 1194.7 | 4732.7 |
| February | -15.9 | 3547.9 | 1198.1 | 4746.0 |
| March | -8.1 | 2777.0 | 937.8 | 3714.8 |
| April | 4.9 | 1492.3 | 503.9 | 1996.2 |
| May | 13.1 | 681.9 | 230.3 | 912.2 |
| June | 19 | 98.8 | 33.4 | 132.2 |
| July | 21.3 | -128.5 | -43.4 | -171.9 |
| August | 17.7 | 227.3 | 76.8 | 304.1 |
| September | 12 | 790.6 | 267.0 | 1057.6 |
| October | 2.8 | 1699.8 | 574.0 | 2273.8 |
| November | -5.9 | 2559.6 | 864.3 | 3424.0 |
| December | -12.6 | 3221.8 | 1087.9 | 4309.7 |

The required amount of fresh air proportionally depends on number of occupants in space. The amount of ventilation air can be found according to following equation:

$$V = N * 5$$

Where

V is ventilation air (CFM);

N is number of occupants in space;

5 is recommended ventilation rate is 5 CFM/person [based on Ashrae Standard (2003)].

Then the heat loss estimation from infiltration is:

$$Q_{vent} = V \cdot \rho_{air} \cdot c_p \cdot (T_{in} - T_{out}) \cdot 60 \quad (3.3)$$

where

$Q_{vent}$ is heat load in Btu/hr;

V is volumetric airflow rate in cfm;

$\rho_{air}$ is the density of the air in lbm/ft$^3$;

$c_p$ is specific heat capacity of air at constant pressure in Btu/lbm –F;

$T_i$ is indoor air temperature in °F;

$T_o$ is outdoor air temperature in °F;

The heat capacity of air is product of $c_p$ and $\rho_{air}$, and is equivalent to 0.018 Btu per (°F) ($ft^3$) (Bhatia, nd).

### 3.3.3. Total Heat load

The total heat load will consist of these two conductive and convective heat losses explained above. However, a person in average generates energy at a rate of 400 Btu/h, which is equivalent to 0.117 kW (Tiernan, 1997). Therefore, the total head load for geothermal unit decreases as the number of people increases in the shelter, due to the amount of additional heat extracted by them. Then in order to calculate the amount of heat load to be provided by GSHP, the rate of energy extracted from people is subtracted from total heat load, yielding overall heat load changing in accordance with number of occupancies. Table B1 in Appendix B shows the results of heat load calculations for each month depending on average outside temperature (taken from Astana weather station), and considering the average people load by time during the day, based on results of experiment explained earlier.

It can be noticed, that during February the heat load reaches its peak of approximately 5 kW. This is the amount of heat that must be provided in order to keep the shelter's inside temperature at constant 20 ℃.

## 4. Implementation and Integration chapter

### 4.1. Thermal load simulation results

At this point, RETScreen is used to propose the best proportion of GSHP and electric heater. After that, the amount of electricity required for electric heater and geothermal pump

in that proportion will be calculated, and added to total electricity consumption of the shelter (for illumination, wi-fi and etc.), and considered as total electricity load of the shelter. Then this electric load will be given to HOMER, to obtain best combination of energy sources (solar, wind or grid) in terms of economics to provide that amount of electricity.

RETScreen 4 is effective in examining a potential green energy projects for the technical and financial feasibility. Besides, climate data location provided by National Aeronautics & Space Administration's (NASA) Langley Research Center are already integrated in the software. Therefore the weather conditions data for the city of Astana were selected directly in the software (refer to Figure 4.1). In addition, the program offers several methods of investigation that are sorted by the type of projects they suit most. For example, the heating type project would consist of five standard steps of analyzing: Energy Model, Cost Analysis, Emission Analysis, Financial Analysis, and Sensitivity & Risk Analysis. Since the goal is to investigate feasibility of installing geothermal heating system instead of conventional electric heaters, the type of the project is left as heating project.

| | Unit | Climate data location | Project location |
|---|---|---|---|
| Latitude | °N | 51,1 | 51,1 |
| Longitude | °E | 71,4 | 71,4 |
| Elevation | m | 350 | 350 |
| Heating design temperature | °C | -28,2 | |
| Cooling design temperature | °C | 29,9 | |
| Earth temperature amplitude | °C | 28,9 | |

| Month | Air temperature | Relative humidity | Daily solar radiation - horizontal | Atmospheric pressure | Wind speed | Earth temperature | Heating degree-days | Cooling degree-days |
|---|---|---|---|---|---|---|---|---|
| | °C | % | kWh/m²/d | kPa | m/s | °C | °C-d | °C-d |
| January | -14,1 | 77,3% | 0,98 | 98,4 | 4,2 | -15,3 | 995 | 0 |
| February | -14,3 | 75,8% | 1,84 | 98,4 | 4,3 | -15,0 | 904 | 0 |
| March | -7,7 | 78,4% | 3,37 | 98,3 | 4,4 | -9,5 | 797 | 0 |
| April | 5,1 | 64,0% | 4,65 | 97,9 | 4,2 | 3,8 | 387 | 0 |
| May | 13,7 | 54,7% | 5,94 | 97,4 | 4,1 | 17,4 | 133 | 115 |
| June | 19,3 | 53,8% | 6,50 | 97,0 | 3,7 | 23,3 | 0 | 279 |
| July | 20,5 | 59,6% | 6,06 | 96,8 | 3,3 | 24,1 | 0 | 326 |
| August | 18,3 | 58,5% | 5,10 | 97,0 | 3,3 | 21,5 | 0 | 257 |
| September | 12,2 | 59,2% | 3,73 | 97,6 | 3,6 | 13,9 | 174 | 66 |
| October | 4,2 | 68,0% | 2,23 | 98,0 | 4,0 | 4,1 | 428 | 0 |
| November | -5,9 | 79,1% | 1,25 | 98,4 | 4,1 | -7,1 | 717 | 0 |
| December | -12,2 | 78,4% | 0,82 | 98,4 | 4,4 | -13,8 | 936 | 0 |
| **Annual** | 3,4 | 67,2% | 3,55 | 97,8 | 4,0 | 4,1 | 5 472 | 1 043 |
| Measured at | m | | | | 10,0 | 0,0 | | |

Figure 4.1. Climate data location for Akmola (RETScreen, 2015)

First of all, the load of the project needs to be identified properly. It is important to consider that the program was designed to perform feasibility analysis for residential areas with the space of approximately 30 $m^2$ per person. For that reason, heated floor area value for building was taken as 63 $m^2$ instead of available 25 $m^2$ for bus station in order to match the total peak heating load of 5kW. Heating load for building was selected according to Building Heating Load Chart shown in Figure 4.2. For the heating design temperature of -28.2°C and a construction with medium insulation that value equals to 80 $W/m^2$. Electric heaters which are chosen to be the base case heating system consume the electric energy to generate the same amount of thermal energy. This means that the base case heating system has 100 percent efficiency. As it is shown in Table 4.1, the day time cost for electricity in Astana city is 0.08$/kWh. Since the bus station is planned to operate from 6:00 to 00:00, the cost for electricity during the night time is not considered.

Heat pumps that consume the same amount of energy as electric heaters but 3.5 times more efficient are proposed as a clean energy alternative in the Energy Model section. Since the total peak heating load of the system is 5kW, then 5kW capacity heat pump could serve all the thermal load of the building. In that case any peak load heating system would not be required, because there would be no remaining heating needs. This is true if the bus station heating will not be provided with any back-up. The probability that the heating system will totally fail is assumed to be negligible. Moreover, even in the case of failure, the waiting time until the heating system is repaired assumed to be acceptable. Therefore, it was decided to exclude back-up system for thermal load from the system design. However, there is a possibility that combined geothermal and electric heater system will demonstrate more optimistic results. For that reason, feasibility analysis was performed for a range of possible heat pump capacities, so that the remaining thermal load would be supplied by conventional electric heaters. Five different system design graphs are illustrated in Figure 4.3.

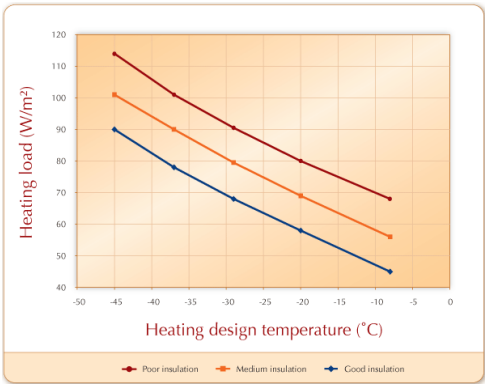


Figure 4.2. Building Heating Load Chart (RETScreen, 2015)

Table 4.1. Differentiated rates for electric energy (Ezez, 2016)

| | |
|---|---|
| Night time (23:00 – 07:00) | 0.018$ per kWh |
| Day time (07:00 – 23:00) | 0.080 per kWh |

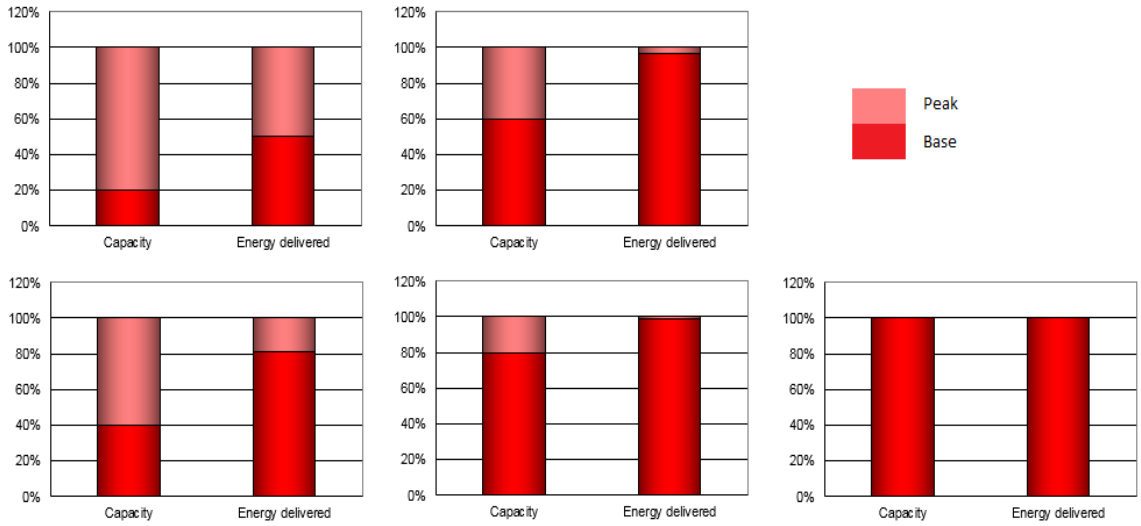


Figure 4.3. System design graphs for five different cases

During cost analysis, the model requires initial, annual and periodic costs for proposed system. In addition, the money that would have been spent in the base case is considered as credit savings and taken into account during Net Present Value calculation.

Although geothermal technologies benefit in terms of long period operating costs due to energy consumption efficiency, the installation costs including mobilization and commissioning are significantly higher than the costs for conventional systems. According to BRE's Sustainable Energy Centre, the average total system initial cost is 1242.7 per kW (EST, 2004). Whereas, conventional electric heaters cost only 60$ per kW currently on market. Annual expenses both for ground source heat pump and electric heaters are negligible. Regarding periodic costs, the compressor in geothermal system requires replacement every 15 years and electric heater is likely to have a lifespan of 10 years (ibid). Replacing compressor and circulating pump costs about 800$ (CAT Information Service, 2016). Furthermore, 5% of allowance permitted for contingencies and a delay for about a month is required for construction works.

Consumption of ground source renewable energy also contributes to an annual reduction in greenhouse gas emission (GHG). Even if this reduction does not bring any financial benefit, as it was mentioned before, it is an important aspect and one of the primary goals of the project. Greenhouse gas emission in Kazakhstan per MWh is 0.403 tons of carbon dioxide with 7% of transmission and distribution losses (Indexmundi, 2016).

| | | |
|---|---|---|
| **General** | | |
| Fuel cost escalation rate | % | 5,0% |
| Inflation rate | % | 8,0% |
| Discount rate | % | 8,0% |
| Project life | yr | 25 |
| **Finance** | | |
| Incentives and grants | $ | 0 |
| Debt ratio | % | 50,0% |
| Debt | $ | 1 242 |
| Equity | $ | 1 242 |
| Debt interest rate | % | 4,00% |
| Debt term | yr | 5 |
| Debt payments | $/yr | 279 |

Figure 4.4. Financial Input Parameters into the RETScreen 4

The figure above shows input financial parameters of the model. Mean inflation and discount rates for last five years is 8% (Trading Economics, 2016). The debt ratio is assumed to be 50% and the debt term was set to 5 years in order to analyze the feasibility of payback.

Table 4.2 shows financial viability parameters for each of the system design cases. The feasibility analysis results are compared according to internal rate of return, payback period, net present value, net benefit to cost ratio and the annual reduction in impure emissions. According to the table, the internal rate of return in each cases exceeds the required rate of return, thus in terms of IRR, the design configurations are in acceptable range. There are only two cases that have payback periods less than the established debt term of 5 years: applying 1kW and 2kW capacities of heat pumps. However, the simple payback method is only the measure of time used for indication of the investment recovery. Lower payback period does not mean that the project is more profitable compared to another. Net Present Value is the worth of all future cash flows, discounted at the given discount rate in the present price of currency. The proportion of 60% geothermal unit and 40% electric heaters is the most profitable in terms of NPV, although its payback period is longer. The model also calculates the ratio of the net benefit to costs of the project. In addition, the annual reduction in GHG emission obviously increases in accordance with capacity of renewable energy heating system. Considering mentioned financial parameters, *2kW heat pump and 3kW electric heater* configuration was chosen as the most technically and financially efficient.

Table 4.2. Financial viability of all the five proposed cases obtained

| | | 20%Base | 40%Base | 60%Base | 80%Base | 100%Base |
|---|---|---|---|---|---|---|
| | | 80%Peak | 60%Peak | 40%Peak | 20%Peak | |
| Pre-tax IRR -equity | % | 41.4 | 33.3 | 26.1 | 20.0 | 16.2 |
| Pre-tax IRR - assets | % | 24.1 | 20.1 | 16.3 | 12.6 | 10.1 |
| After-tax IRR -equity | % | 41.1 | 33.3 | 26.1 | 20.0 | 16.2 |
| After-tax IRR -assets | % | 24.1 | 20.2 | 16.3 | 12.6 | 10.1 |
| Simple payback | yr | 3.9 | 4.8 | 6.1 | 8.0 | 9.8 |
| Equity payback | yr | 3.0 | 4.1 | 5.5 | 6.9 | 8.3 |
| Net Present Value (NPV) | $ | 3717 | 6159 | 6798 | 5982 | 5069 |
| Annual life cycle savings | $/yr | 348 | 577 | 637 | 560 | 475 |
| Benefit-Cost (B-C) ratio | - | 6.99 | 5.96 | 4.65 | 3.41 | 2.63 |
| Debt service coverage | - | 2.37 | 1.93 | 1.53 | 1.17 | 0.95 |
| Annual reduction | $tCO_2$ | 1.7 | 2.8 | 3.3 | 3.4 | 3.4 |

### 4.2. Electric load

As it was mentioned before, the HOMER gives us best combination of energy sources prioritizing by Net Present Cost for the system. However, from renewable energy sources, HOMER is designed to recognize solar and wind energies only, but not geothermal unit. Therefore, it was decided to separate heat and electric loads of the shelter.

In designed bus shelter, the electric energy is consumed mainly by illumination, wi-fi router and the light box. According to “DivoSvet” LED Technology manufacturer’s pricelist, a common LED lamp consumes energy at a rate of 36W, Energy Use calculator approximates the energy rate of usage for wi-fi router to be 6W, and Red and Led manufacturers of light box estimate its rate to be 22W. In addition to these electric loads, the load of heating system should be added, which is the combination of GSHP and electric heater. As it was proposed by our thermal load analysis, the best solution in terms of NPV and Payback Period is to provide heat load to the shelter by Ground Source Heat Pump and electric heater in proportion of 2kW and 3kW respectively. Therefore, in order to provide

40% of heat load, with 350% efficient GSHP, 3.5 times less electricity will be required. Other 60% of heat provision must be supplied by conventional electric heaters with 100% efficiency. Table B2 represents values of total electric load, already including the electricity consumption of heating system.

### 4.3. Electric load simulation results

The major part of working with HOMER micro power optimization model is gathering required input information. Firstly, weather data have to be collected accurately in order to receive realistic results from the wind and PV array power estimations. The monthly averages of wind speed according to the site evaluation were entered into HOMER. Variation with height also taken into consideration. The surface roughness length is chosen to be 1.5, because the selected installation area is the city side space without any tall obstacles. The resource inputs to calculate the PV array power are adopted from a hybrid smart house project for the city of Astana that also used the solar renewable energy (Kazamaganbetova et al., 2015). From economical aspect of the project, annual interest rate needs to be taken into account. The mean annual interest rate for last five years in Kazakhstan is 8% (Trading Economics, 2016).

Table 4.3. Table of monthly average power generation from PV array

| Month | Clearness Index | Daily Radiation (kWh/m2/d) |
|---|---|---|
| January | 0.536 | 1.186 |
| February | 0.617 | 2.259 |
| March | 0.640 | 3.813 |
| April | 0.558 | 4.774 |
| May | 0.566 | 5.996 |
| June | 0.583 | 6.717 |
| July | 0.567 | 6.262 |
| August | 0.554 | 5.157 |
| September | 0.578 | 3.944 |
| October | 0.478 | 2.070 |
| November | 0.521 | 1.317 |
| December | 0.474 | 0.856 |
| Average: | 0.566 | 3.702 |

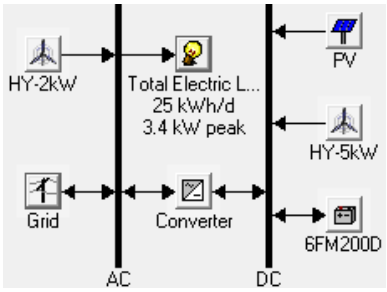


Figure 4.5. Components of electric load simulation model

The electric load studied here is the total electric load to run the bus shelter, which includes heating system, illumination, Wi-Fi and light box loads. The costs for each type of equipment are shown in Table 4.4.

Table 4.4. Equipment costs

| | Size (kW) | Capital ($) | Replacement ($) | O &M ($/yr) | Lifetime (years) |
|---|---|---|---|---|---|
| PV array | 0.245 | 250 | 250 | 3 | 25 |
| Converter | 0.600 | 170 | 170 | 0 | 20 |
| | Quantity | | | | |
| HY-5kW Wind Turbine | 1 | 5500 | 5500 | 83 | 15 |
| HY-2kW Wind Turbine | 1 | 3000 | 3000 | 45 | 15 |
| Vision 6FM200D Battery | 1 | 400 | 400 | 0 | - |

Certain constraints have to be given to the model in terms of sizing of equipment. For example, the maximum capacity allowed for PV array is set to be 5kW, because a PV panel with capacity of 200W occupies 1 $m^2$ of space (The Eco Experts, 2016), while we have only 25$m^2$ available on the roof of the station. To test what capacities of wind turbines are suitable, two types of turbines were added to the system. The wind turbine types were selected to match the capacities under consideration and the costs were taken accordingly. The batteries are also included into the model to consider the possibility of excessive electricity generation. Furthermore, PV, wind turbine and battery installations have DC

output current. Therefore, the model cannot be run without a converter. Table 4.5 demonstrates the search space with all the equipment sizes that are considered in the model.

Differentiated rates for electric energy are inputted for night and day time into the grid parameters (see Table 4.1).

Table 4.5. Search Space in HOMER model

| | PV Array (kW) | XLS (Quantity) | AIR (Quantity) | Grid (kW) | 6FM200D (Quantity) | Converter (kW) |
|---|---|---|---|---|---|---|
| 1 | 0.000 | 0 | 0 | 1,000.000 | 0 | 0.00 |
| 2 | 1.000 | 1 | 1 | | 1 | 1.00 |
| 3 | 2.000 | 2 | 2 | | 2 | 2.00 |
| 4 | 3.000 | 3 | | | 3 | 3.00 |
| 5 | 4.000 | 4 | | | 4 | 4.00 |
| 6 | 5.000 | 5 | | | 5 | 5.00 |
| 7 | | | | | 6 | 6.00 |
| 8 | | | | | 7 | 7.00 |
| 9 | | | | | 8 | 8.00 |

Moreover, there are sellback rates for excessive green energy electricity that can be sold back to the grid. The sellback rates are shown in Table 4.6 below.

Table 4.6. Sellback rates (Rfc. Kegoc, 2016)

| | |
|---|---|
| Night time (23:00 – 07:00) | 0.066 $ per kWh |
| Day time (07:00 – 23:00) | 0.101 $ per kWh |

The table above shows the categorized rankings with the least-cost system of each type. Categorization is convenient to analyze the results, rather than reading the outcomes of all the 10692 simulations. The table states that the renewable energy technologies are not economically feasible for this type of project.

Table 4.7. Electric load optimization results

| PV (kW) | XLS | AIR | 6FM200D | Conv. (kW) | Grid (kW) | Initial Capital | Operating Cost ($/yr) | Total NPC | COE ($/kWh) | Ren. Frac. |
|---|---|---|---|---|---|---|---|---|---|---|
| | | | | | 1000 | $ 0 | 666 | $ 7,109 | 0.073 | 0.00 |
| 1 | | | | 1 | 1000 | $ 1,304 | 578 | $ 7,469 | 0.077 | 0.15 |
| | | | 1 | 1 | 1000 | $ 683 | 691 | $ 8,064 | 0.083 | 0.00 |
| 1 | | | 1 | 1 | 1000 | $ 1,704 | 600 | $ 8,111 | 0.084 | 0.15 |
| | 1 | | | | 1000 | $ 3,000 | 621 | $ 9,627 | 0.099 | 0.23 |
| 1 | 1 | | | 1 | 1000 | $ 4,304 | 529 | $ 9,946 | 0.103 | 0.36 |
| | 1 | | 1 | 1 | 1000 | $ 3,683 | 646 | $ 10,582 | 0.109 | 0.23 |
| 1 | 1 | | 1 | 1 | 1000 | $ 4,704 | 551 | $ 10,588 | 0.109 | 0.36 |

## 4.4. Geothermal unit

### 4.4.1. Soil analysis

In order to estimate the length of pipes in our geothermal system we need to calculate the undistributed underground temperature distribution. This process is divided into two steps: soil analysis and thermal analysis. Soil analysis allows us to investigate thermal properties of the ground in Astana. Whereas, thermal analysis will finally show the required underground temperature distribution.

The process of soil analysis was complicated by several factors such as lack of information and equipment in order to conduct soil investigation study. Therefore, it was important to make several assumptions in order to simplify the process and ultimately make obtainment of results even possible.

1. Density is the most important characteristic of the soil layers, as it was the only available one.

2. Thermal properties of the soil are dependent on the density of the layer only.

The description of soil layers was obtained from a geo-engineering report in Astana (Ospanova, 2012). The densities of the layers were found and the corresponding thermal

properties were looked up in ASHRAE HVAC Handbook (2011). The results of the soil analysis for each soil layer can be observed in Table 4.8.

Table 4.8. Densities and thermal properties of each soil layer.

| Depth (m) | Description of the soil | Density ($kg/m^3$) | Thermal conductivity ($W/m \cdot K$) | Thermal diffusivity ($mm^2/s$) |
|---|---|---|---|---|
| 0-1 | clayed soil with crushed stone | 2100 | 1.3 | 0.65 |
| 1-2 | high-plastic clayed soil | 1750 | 0.86 | 0.52 |
| 2-3 | semi-solid clayed soil | 1950 | 0.86 | 0.52 |
| 3-5 | high-plastic clayed soil | 1750 | 0.86 | 0.52 |
| 5-7 | clayed soil with layers of sand | 1750 | 0.86 | 0.52 |
| 7-9 | gravel sand | 1500 | 0.35 | 0.28 |
| 9-11 | gravel soil | 2100 | 1.3 | 0.65 |
| 11-14 | gravel sand and clay | 1600 | 0.86 | 0.52 |
| 14-17 | clayed soil with crushed stone | 1950 | 0.86 | 0.52 |

### 4.4.2. Thermal analysis

After thermal characteristics of the soil in Astana were found, the underground temperature distribution was calculated. For this purpose, the equation of undistributed ground temperature (Xing, 2014) was utilized in Excel:

$$T_s(z,t) = T_{s,avg} - \sum_{n=1}^{2} e^{-z\sqrt{\frac{n\pi}{a_s t_p}}} T_{s,amplitude,n} cos\left[\frac{2\pi n}{t_p}(t - PL_n) - z\sqrt{\frac{n\pi}{a_s t_p}}\right] \quad (4.1)$$

where

$T_s(z,t)$ is the undistributed soil temperature at the depth $z$ and time $t$ of the year, in °C;

$z$ is the soil depth, in $m$;

$t$ is the time of year, starting from January 1, in days;

$t_p$ is the period of soil temperature cycle (365), in days;

$a_s$ is the soil diffusivity, $m^2$/days;

$T_{s,avg}$ is the annual average soil temperature, in °C;

$T_{s,amplitude,n}$ is the $n^{th}$ order surface amplitude, in °C;

$PL_n$ is the phase angle of the annual soil temperature cycle, in days.

The values used in Equation (4.1) for Astana can be found in Table 4.9.

Table 4.9. Constants for underground temperature calculation (ibid).

| $T_{s,avg}$ (°C) | $T_{s,amplitude,1}$ (°C) | $T_{s,amplitude,2}$ (°C) | $PL_1$ (days) | $PL_2$ (days) | $a_s$ ($m^2$/day) |
|---|---|---|---|---|---|
| 5.7 | 13.3 | -1.9 | 31 | 15 | 0.044928 |

By observing the results of thermal analysis, we can see that after the depth of 10m the underground temperature remains constant with very little fluctuations throughout the year at 5.7°C.

### 4.4.3. Piping material

BRE's Sustainable Energy Centre states, that the right choice of piping material affects the life, cost, pumping energy and heat pump performance. The most common material worldwide is high-density polyethylene (HDPE), since it is flexible and can be easily heat fused. In addition, appropriate diameter of the tubes must be chosen, so that it is large enough to keep the pumping power small, but at the same time, small enough to cause turbulent flow in order to reach good heat transfer level.

### 4.4.5. Circulating fluid

Circulating fluid is the fluid running through the loop, and gaining heat in order to give it to the heat pump. The freezing point of this fluid must be below the mean temperature of the heat pump. Since the mean temperature of the heat pump can be as low as -4 degrees, the antifreeze solution must be added to prevent freezing. This antifreeze solution should be of good thermal performance even under low temperatures.

### 4.4.6. Pipe length calculation

According to Chiasson (2016), the equation models of the horizontal and vertical loops are the same for calculation of the length. Therefore, the length of the borehole for vertical configuration will be estimated, and then translated into horizontal configuration. The costs of these two loops will be compared, and the best will be chosen.

According to Philippe et al (2010), for the calculation of the total length of the borehole, the sizing equation proposed by Kavanaugh and Rafferty (1997) (contained in ASHRAE Handbook) can be used:

$$L = \frac{q_h R_b + q_y R_{10y} + q_m R_{1m} + q_h R_{6h}}{T_m - (T_g + T_p)} \qquad (4.2)$$

where

$L$ is the total borehole length;

$T_m$ is the mean fluid temperature in the borehole;

$T_g$ is the undisturbed ground temperature;

$T_p$ is the temperature penalty, which represents a correction to the undisturbed ground temperature due to thermal interferences between boreholes (in the case of single borehole is 0);

$q_y$, $q_m$ and $q_h$ represent, respectively, the yearly average ground heat load (thermal annual imbalance), the highest monthly ground load and the peak hourly ground load;

$R_{10y}$, $R_{1m}$ and $R_{6h}$ are effective ground thermal resistances corresponding to 10 years, one month and six hours ground loads; and

$R_b$ is the effective borehole thermal resistance.

This equation assumes that only conduction contributes to the heat transfer, and the moisture evaporation with underground water movement have no significant effects. This equation considers the worst-case scenario represented by three successive thermal pulses with durations corresponding to 10 years, one month and six hours. These values are found from the building loads calculated earlier, and the COP of the heat pump.

Effective ground thermal resistances $R_{10y}$, $R_{1m}$ and $R_{6h}$ account for transient heat transfer between the borehole and undisturbed ground. The values can be found assuming the cylindrical heat source solution, and is only valid for transient heat transfer in radial direction, and axial effects assumed to be negligible. Then the general formula to find these resistances is:

$$R = \frac{1}{k} f(\alpha, r_{bore}) \quad (4.3)$$

$$f = a_0 + a_1 r_{bore} + a_2 r_{bore}^2 + a_3 \alpha + a_4 \alpha^2 + a_5 \ln \alpha +$$

$$a_6 \ln \alpha^2 + a_7 r_{bore} \alpha + a_8 r_{bore} \ln \alpha + a_9 \alpha \ln \alpha \quad (4.4)$$

As it can be seen from the Equations 3.6 and 3.7, function f depends on only two parameters, namely the diffusivity of the ground in $m^2/day$ and the radius of the bore in $m$. The coefficients are provided by the source for the calculation of the $f_{6h}$, $f_{1m}$ and $f_{10y}$. Then, it should be divided by the conductivity of the ground presented above.

Temperature penalty $T_p$ stands for the correction of undisturbed ground temperature due to thermal interference between boreholes. In this case, due to small size of the geothermal unit, single borehole is considered. Therefore, temperature penalty is assumed to be zero.

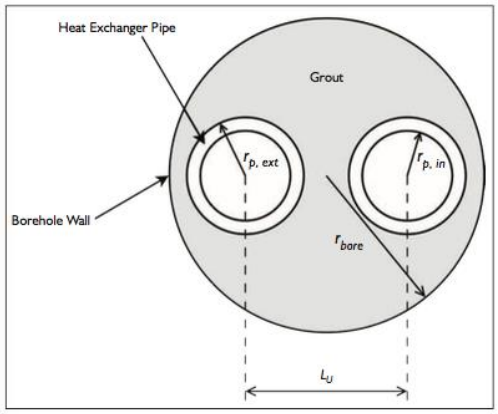


Figure 4.6. Cross-section of geothermal vertical borehole

Figure 4.5 represents a typical single U-tube borehole, filled with grout with high conductivity. The average fluid temperature $T_m$ is assumed to be constant along the depth of the borehole, and equal to the average of the inlet and outlet fluid temperatures to the heat pump. The effective borehole thermal resistance can be calculated from the values of three base effective thermal resistances:

$$R_b = R_g + \frac{R_p + R_{conv}}{2} \quad (4.5)$$

These three resistances $R_{conv}$ , $R_p$ *and* $R_g$ are convective resistance inside each tube, the conduction resistance for each tube and grout resistance respectively, and can be found according to following equations:

$$R_{conv} = \frac{1}{2\pi r_{p,in} h_{conv}} \quad (4.6)$$

$$R_p = \frac{\ln(r_{p,ext}/r_{p,in})}{2\pi k_{pipe}} \quad (4.7)$$

$$R_g = \frac{1}{4\pi k_{grout}} \left[ \ln \frac{r_{bore}}{r_{p,ext}} + \ln \frac{r_{bore}}{L_U} + \frac{k_{grout} - k}{k_{grout} + k} \ln \frac{r_{bore}^4}{r_{bore}^4 - \left(\frac{L_U}{2}\right)^4} \right] \quad (4.8)$$

where

$h_{conv}$ is the film convection coefficient;

$r_{p,in}$ *and* $r_{p,ext}$ are the inner and outer radii of the pipe;

$k_{pipe}$ is the thermal conductivity of the pipe material;

$k_{grout}$ is the thermal conductivity of the grout;

$k$ is the ground thermal conductivity; and

$L_U$ is the center-to-center distance between the two pipes.

Chiasson (2016) states that $q_y$, $q_m$ and $q_h$, representing the ground loads, do not relate to the whole building load, but to heat pump loads through the coefficient of performance through multiplying the building load by factor F:

$$F = \frac{COP - 1}{COP} \quad (4.9)$$

In order to find the ground loads, the concept of load factor (LF) is introduced, which is defined as the ratio of average heat pump load to the peak heat pump load. The load factor for a month and year is expressed as follows respectively:

$$LF_m = \frac{Q_{m,HP}}{\dot{q}_{h,HP} \times (N_m)}, \quad LF_a = \frac{Q_{a,HP}}{\dot{q}_{h,HP} \times (N_a)} \quad (4.10)$$

where

Q is an energy quantity in kWh;

$\dot{q}$ is an energy rate in kW;

N is the number of hours;

And subscript H, h, m and a refer to heat pump, hour, month and annual respectively. Consequently, $Q_a$ represents the total annual heating energy load.

Finally, the required ground loads can be calculated according to following equations:

$$\dot{q}_h = \dot{q}_{h,HP} \times F \quad (3.14), \quad \dot{q}_m = \dot{q}_h \times LF_m \times F \quad (4.11) \quad and$$

$$\dot{q}_a = \dot{q}_{h,htg} \times LF_{a,htg} \times F_{htg} + \dot{q}_{h,clg} \times LF_{a,clg} \times F_{clg} \quad (4.12)$$

Chiasson (2016) also mentions that mean fluid temperature is a critical parameter in calculation of the length of the borehole, as it appears in the denominator of the main equation as a difference term with undisturbed ground temperature. The mean fluid temperature of the pump inlet and outlet, i.e. average fluid temperature in the borehole exchanger, requires a design consideration made by engineers in terms of inlet temperature $T_{in}$. He proposes to choose the inlet temperature 8-11 degrees lower than the undisturbed ground temperature. Then, the mean temperature can be found according to following equation:

$$T_f = T_{in} + \frac{\dot{q}_h}{2\dot{m}c_p} \quad (4.13)$$

As it can be seen from the above equations, the calculation of length of pipes require certain input parameters. Tables 4.10 and 4.11 represent values for all input parameters, and the calculated outputs.

Table 4.10. Spreadsheet for designing geothermal boreholes: set of inputs

| **Set of inputs** | **Notation** | **Units** | **Values** |
|---|---|---|---|
| *Ground loads* | | | |
| peak hourly ground load | $q_h$ | $W$ | 1560 |
| monthly ground load | $q_m$ | $W$ | 32 |
| yearly average ground load | $q_y$ | $W$ | 50 |
| *Ground properties* | | | |
| thermal conductivity | $k$ | $W \cdot m^{-1} \cdot K^{-1}$ | 0.86 |
| thermal diffusivity | $\alpha$ | $m^2 \cdot day^{-1}$ | 0.0449 |
| undisturbed ground temperature | $T_g$ | $°C$ | 5.7 |
| *Fluid properties* | | | |
| thermal heat capacity | $c_p$ | $J \cdot kg^{-1} \cdot K^{-1}$ | 4200 |
| total mass flow rate per kW of peak hourly ground load | $m_{fls}$ | $kg \cdot s^{-1} \cdot kW^{-1}$ | 0.050 |
| *Borehole characteristics* | | | |
| borehole radius | $r_{bore}$ | $m$ | 0.060 |
| pipe inner radius | $r_{pin}$ | $m$ | 0.0137 |

| | | | |
|---|---|---|---|
| pipe outer radius | $r_{pext}$ | $m$ | 0.0167 |
| grout thermal conductivity | $k_{grout}$ | $W \cdot m^{-1} \cdot K^{-1}$ | 1.50 |
| pipe thermal conductivity | $k_{pipe}$ | $W \cdot m^{-1} \cdot K^{-1}$ | 0.42 |
| center-to-center distance between pipes | $L_U$ | $m$ | 0.0511 |
| internal convection coefficient | $h_{conv}$ | $W \cdot m^{-2} \cdot K^{-1}$ | 1000 |

Table 4.11. Spreadsheet for designing geothermal boreholes: set of results

| **Set of results** | **Notation** | **Units** | **Values** |
|---|---|---|---|
| *Calculation of the effective borehole resistance* | | | |
| convective resistance | $R_{conv}$ | $m \cdot K \cdot W^{-1}$ | 0.0116 |
| pipe resistance | $R_p$ | $m \cdot K \cdot W^{-1}$ | 0.0750 |
| grout resistance | $R_g$ | $m \cdot K \cdot W^{-1}$ | 0.0768 |
| effective borehole thermal resistance | $R_b$ | $m \cdot K \cdot W^{-1}$ | 0.12 |
| *Calculation of the effective ground thermal resistance* | | | |
| short term (6 hours pulse) | $R_{6h}$ | $m \cdot K \cdot W^{-1}$ | 0.1160 |
| medium term (1 month pulse) | $R_{1m}$ | $m \cdot K \cdot W^{-1}$ | 0.3488 |
| long term (10 years pulse) | $R_{10y}$ | $m \cdot K \cdot W^{-1}$ | 0.4965 |
| *Total length calculation* | | | |
| average fluid temperature in the borehole | $T_m$ | $°C$ | -7.09 |
| total length of borehole | $L$ | $m$ | **35** |
| total length of the loop pipe | $L$ | $m$ | **70** |

Table 4.11 shows that the proposed length of the borehole is 35 meters, yielding 70 meters of High Density Polyethylene pipes. As it was mentioned above, the driving equations for calculation of both vertical and horizontal loops are the same, which means that the length of horizontal pipes must account for 70 meters as well. The costs of the

vertical and horizontal looping will be the same in terms of pump cost, pipes cost and distribution system cost, but the cost of installation, which requires either boring or making trench in earth depending on the type of loop. Therefore, the cost can only be compared by the cost of earthworks. In Kazakhstani market, making a borehole is twice as expensive as making a trench ("Буровые/Земляные работы", 2017). Therefore, in terms of economics, horizontal geothermal piping is more economical than vertical tubing.

However, it is a known fact that horizontal looping requires more area in comparison with vertical configuration. Then the most optimal trench size in terms of area and with fewer fittings for the pipes should be proposed. The design choice is a trench of 5 meters in length and 0.65 meters in width in order to fit 14 tubes each 5 meters in length. Since there is sufficient area near the bus shelter available for trenching, our case proposes horizontal piping of geothermal unit. The depth of the trench is chosen to be 10 meters, since the undisturbed ground temperature at that depth reaches the constant value throughout the year regardless of the season changes in the atmosphere. The final configuration model of the horizontal loop can be viewed in our 3D CAD.

### 4.4.7. Cost of geothermal unit

The costs of geothermal unit will consist of expenditures for heat pump, pipes, distribution system, and excavation process for making a trench for the loop in the earth. The cost of 2kW heat pump ranges from 800 to 12000 US dollars in the market, while the price for high density polyethylene tube of required diameter starts from 1.36 USD (400 tg) per meter. Therefore, approximate amount of expenditure for the tube would be 125 USD (41,000 tg). The cost estimation was taken from the pricelist of one of the Kazakhstani polyethylene tubes production company "Plast Invest Production" (2017) located in Almaty. Finally, the average price for making 1 cubic meter of trench in earth costs around 22 USD (7000 tg) ("Буровые/Земляные работы", 2017). Trench size of 5m X 0.65m X 10m =32.5 cubic meters of earth can be removed for 700 US dollars. Distribution system will be forced air ductwork, running air gained heat from pump, and distributing to space through registers.

The cooled space air will return to duct through diffusers, and then is cleaned before the process starts again. The system approximately costs 500 US dollars. The final cost of geothermal unit can be summarized to be *2500 US* dollars in total.

## 4.5.Project management

### 4.5.1. Construction schedule and cost analysis

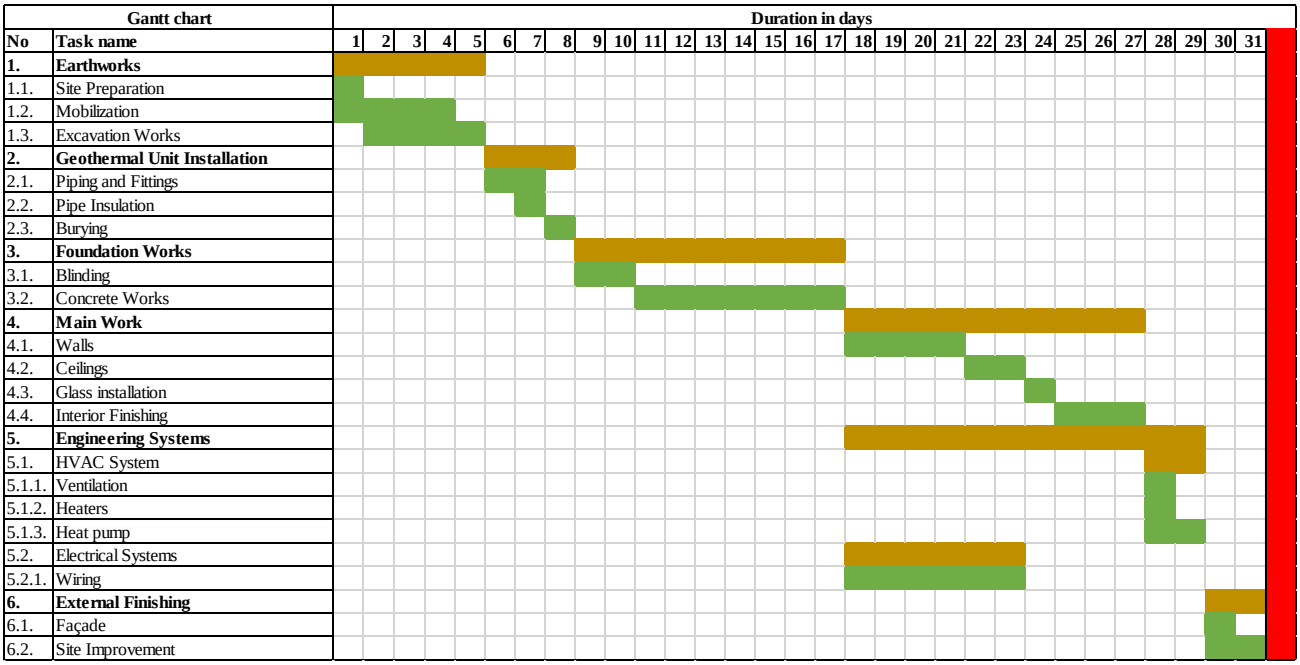


Figure 4.7. Construction Gantt Chart

As it can be seen in the Gantt chart the total duration of the construction will last for 31 days. The start to start and start to finish relations between operations are also demonstrated in the chart.

The costs for equipment, materials and labor for each operation during construction are shown in Table 4.12. All the costs were evaluated according to the prices of Kazakhstani market.

Table 4.12. Construction cost estimation

| No | Task name | Equipment cost ($) | Material cost ($) | Labour cost ($) |
|---|---|---|---|---|
| **1.** | **Earthworks** | | | |
| 1.1. | Site Preparation | 40 | | 160 |
| 1.2. | Mobilization | 500 | | 240 |
| 1.3. | Excavation Works | 750 | | |
| **2.** | **Geothermal Unit Installation** | | | |
| 2.1. | Piping and Pittings | 60 | 125 | 80 |
| 2.2. | Pipe Insulation | | 10 | 160 |
| 2.3. | Burying | 160 | | 80 |
| **3.** | **Foundation Works** | | | |
| 3.1. | Blinding | | 400 | 160 |
| 3.2. | Concrete Works | 160 | 485 | 240 |
| **4.** | **Main Work** | | | |
| 4.1. | Walls | | 960 | 160 |
| 4.2. | Ceilings | | 640 | 160 |
| 4.3. | Glass installation | | 2000 | 160 |
| 4.4. | Interior Finishing | | 400 | 160 |
| **5.** | **Engineering Systems** | | | |
| 5.1. | HVAC System | | | 80 |
| 5.1.1. | Ventilation | | 500 | 80 |
| 5.1.2. | Heaters | | 180 | 80 |
| 5.1.3. | Heat pump | | 1200 | 160 |
| 5.2. | Electrical Systems | | 20 | 80 |
| 5.2.1. | Wiring | | 10 | 80 |
| **6.** | **External Finishings** | | | |
| 6.1. | Façade | | 100 | 160 |
| 6.2. | Site Improvement | | 100 | 240 |
| | Total cost | 1670 | 7130 | 2720 |
| | Total construction cost | 11520 | | |

### 4.5.2. Risk analysis

The extent of applying geothermal green energy technology was mainly selected according to equity payback and net present value. Therefore, it is essential to perform a risk analysis on these two mentioned financial indicators. The risk is dependent on such parameters as initial costs, electrical energy cost in Kazakhstan and debt factors. Hence, the ranges in which these parameters may change have to be accurately specified. In order to assess the risk RETScreen 4 evaluation tool was used.

Although for now, the initial costs of the project are known, the exact date the project will be actualized is indefinite and costs may change due to inflation. Therefore, the range of 20% is allowed for the value of initial costs due to the factors such as value-added tax for import sales, inflation, and high demand for a product. Another important variable is the cost for electricity. During the last 5 years, according to Central-Asian Electric Power Corporation, the price for electricity in the regions of Kazakhstan has not altered for more than 15% (АО "ПАВЛОДАРЭНЕРГО", 2017). Regarding the debt factors, the ranges for debt ratio, interest rate and term were selected as 10%, 15% and 5% respectively. The debt for the project is not a fixed value, but dependent of the designer`s decision as well. Moreover, this particular project is a public service and expected to be funded by the government.

| Parameter | Unit | Value | Range (+/-) | Minimum | Maximum |
|---|---|---|---|---|---|
| Initial costs | $ | 2 484 | 20% | 1 987 | 2 980 |
| Fuel cost - proposed case | $ | 370 | 15% | 314 | 425 |
| Fuel cost - base case | $ | 883 | 15% | 750 | 1 015 |
| Debt ratio | % | 50% | 10% | 45% | 55% |
| Debt interest rate | % | 4,00% | 15% | 3,40% | 4,60% |
| Debt term | yr | 5 | 5% | 4,75 | 5,25 |

Figure 4.8. Ranges for parameters affecting the risk

The Figures 4.8 and 4.9 below show how and to what extent the discussed parameters affect the equity payback and net present value. The parameters are sorted from the most influential to the lowest. The negative value indicates the reverse impact, for example the less the cost for electricity consumed by electric heaters, the longer payback period we get. The same parameter, however, has a positive impact on the net present value. Obviously, the fact that the geothermal unit consumes much less electrical energy than electric heaters due to its efficiency has to be taken into consideration.

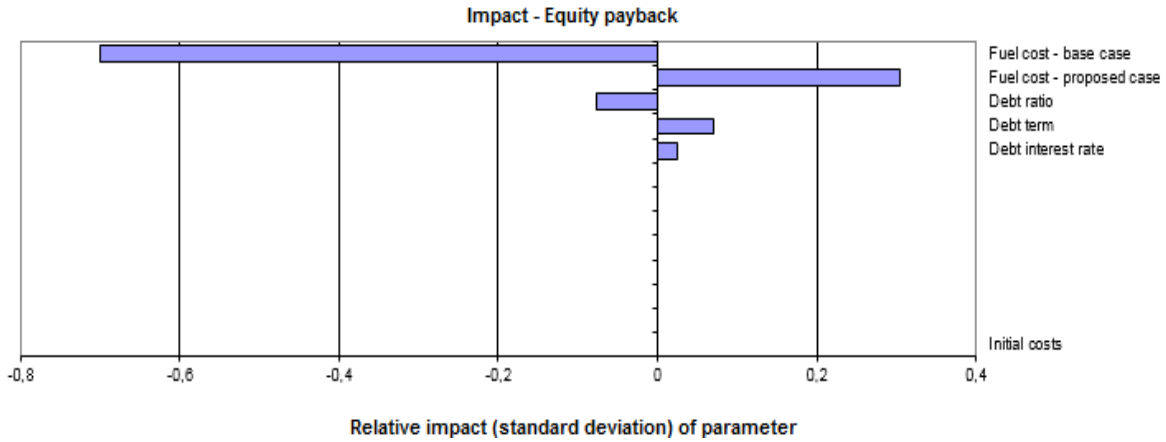


Figure 4.9. Impact graph analyzed on Equity payback

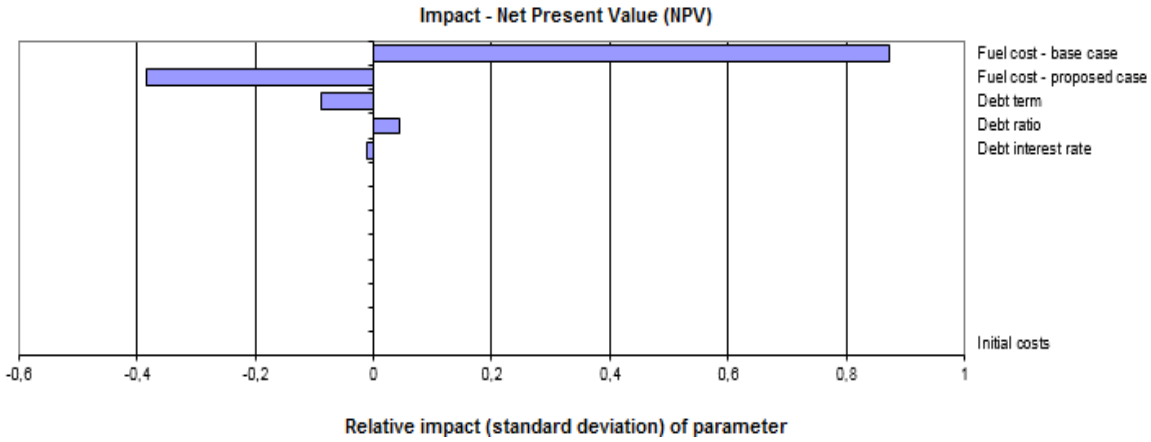


Figure 4.10. Impact graph analyzed on Net Present Value

Generally, the risk assessment proves the strong potential of the proposed green energy technology. The acceptable level of risk for both equity payback and net present value is assumed 5%. Regarding the equity payback, by the known median of 4.1 years, the minimum and maximum within level of confidence are 0.2 and 5.3 years respectively. As it can be seen from the figure below, the probability that the equity payback will exceed the period of 5 years is very unlikely.

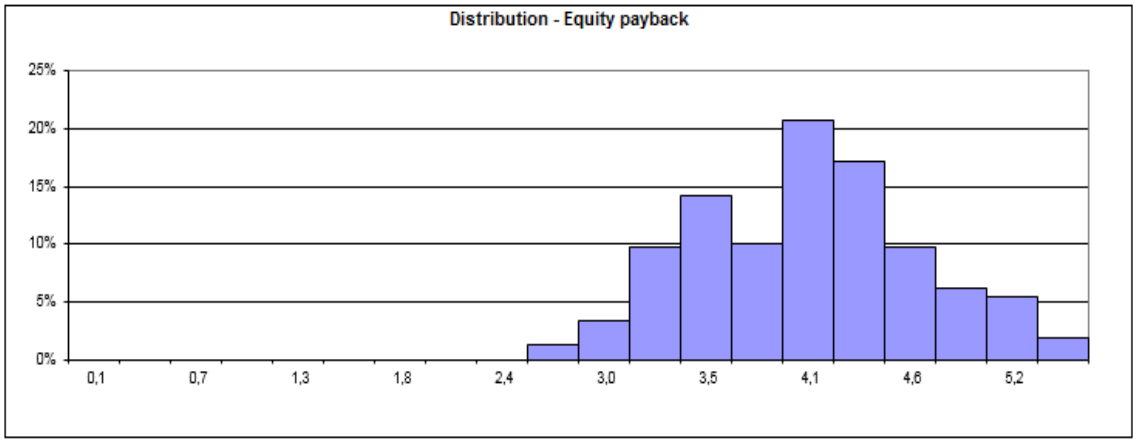


Figure 4.11. Distribution graph analyzed on Equity payback

The net present value most probably will be in the expected range between 5700 and 6800 USD. The risk for getting unacceptably low net present value is even less than 4 %. The distribution chart for net present value is demonstrated below.

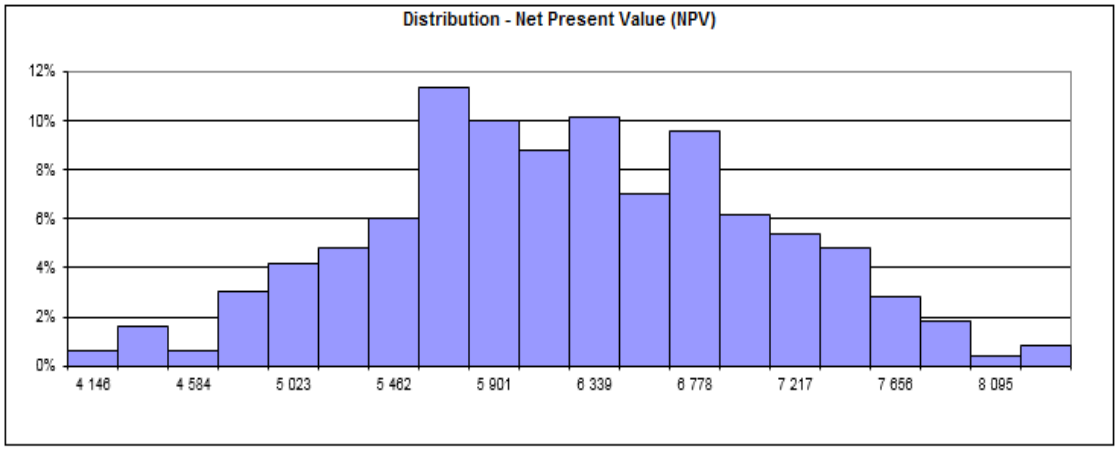


Figure 4.12. Distribution graph analyzed on Net Present Value

### 4.6. Comparison of current technology with proposed technology

The expected lifetime of the project is 25 years. Application of geothermal unit guarantees the positive net present value of at least 5500 USD considering the risk. The most probable profit at the end of the project due to savings from electrical energy is 6159 USD. In addition, it is expected that in 4 years the owner of the project will recoup the initial investment out of the project cash flows generated. In comparison with the current technology, the proposed project is financially beneficial. More importantly, application of a green energy technology will reduce carbon dioxide gas emission by 2.8 tons annually, which was previously discussed. Additional comparison parameters can be found in Table 4.13.

The schematic comparison of the existing technology and the suggested one can be seen in Figure 4.12.

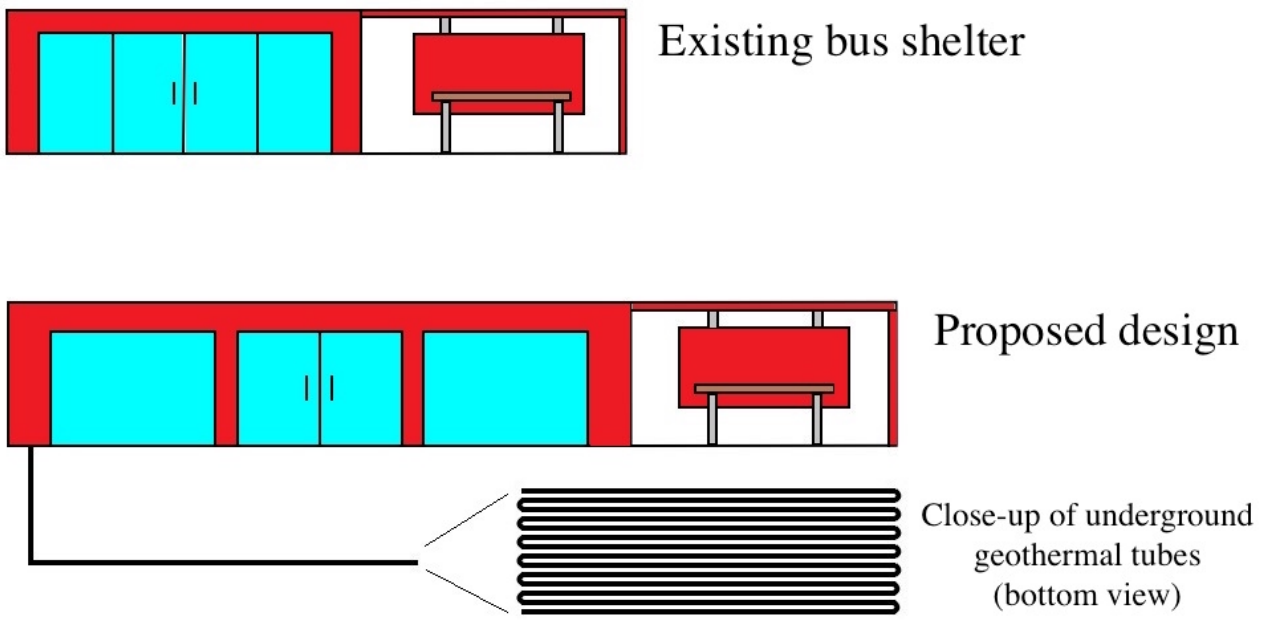


Figure 4.13. Schematics of the existing and proposed bus shelter designs

Table 4.13. Comparison factors for the suggested design

| | Existing design | Proposed design |
|---|---|---|
| Total initial cost | $30000 | $11520 |
| Energy savings | $0 | $6159 |
| Sheltered area | $12m^2$ | $25m^2$ |
| Capacity | 25 passengers | 50 passengers |
| Annual GHG emission | 4.8 $tCO_2$ | 2 $tCO_2$ |

### 4.7. 3D CAD model of the proposed shelter

3D model of the shelter illustrating the geothermal loop configuration was drawn on SolidWorks software. Following Figures 4.13 and 4.14 are isometric view of the shelter and top view of the horizontal loop respectively. Other images of the model can be found in Appendix D.

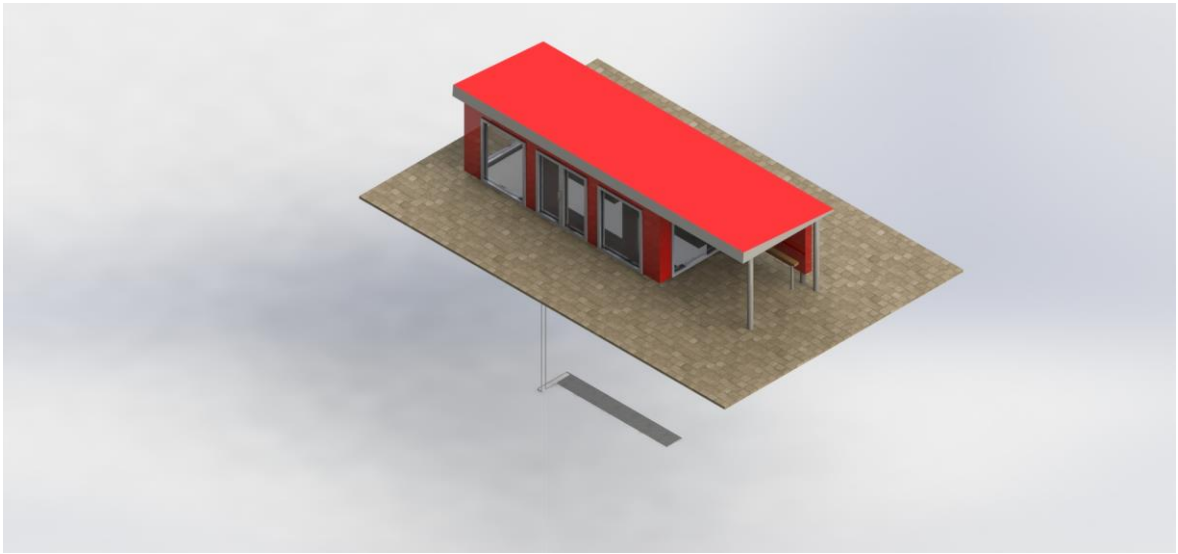

Figure 4.14. Isometric view of shelter CAD

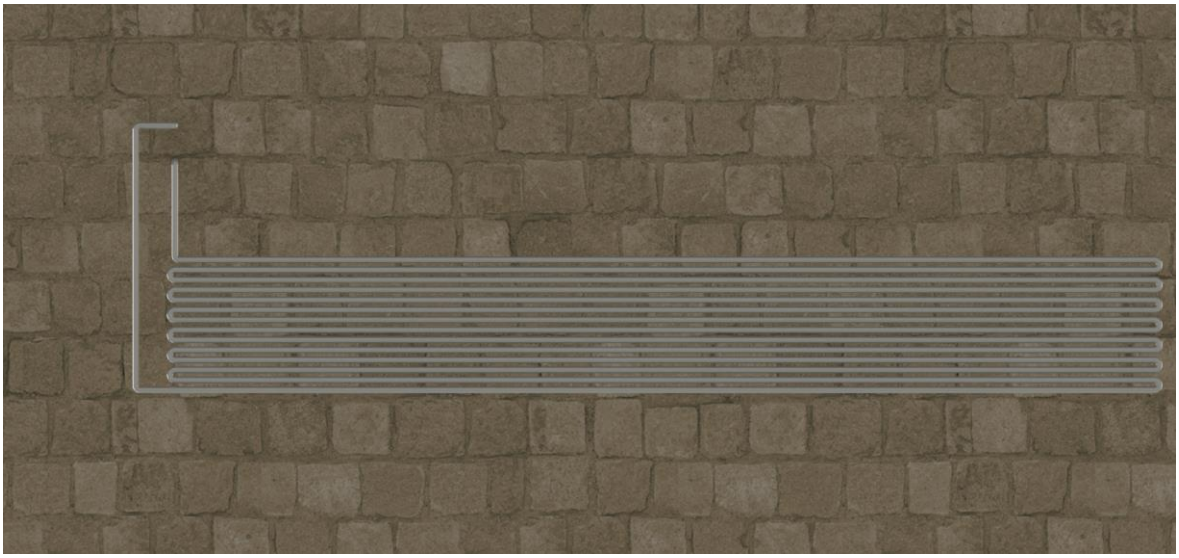

Figure 4.15. Bottom view of horizontal loop

## 5. Concluding remarks

The objective of the project was to improve the current "warm" bus shelter constructions in several aspects: cost, use of conventional energy and space required. For this purpose, the site at "Cardiac Surgery Center" bus stop was chosen for modernization, and further site verification was carried out in SketchUp and Pheonics VR. It showed that the site is suitable for implementation of solar and wind power generation. Then, the passenger load through the day was counted in a field survey, which showed that the new bus station should have at least 25m$^2$ area to accommodate most of the passengers.

For the next step, three green energy technologies: GSHP, PV arrays, and Wind Turbines were tested for technical and financial viability. Firstly, GSHP and conventional electric heater system were compared to fulfill the shelter`s thermal load using RETScreen decision supporting tool. The design combination of 40% GSHP and 60% electric heater demonstrated the most optimistic viability in terms of net present value of the project. Then the electric load of the proposed design, which included electric heaters, illumination, Wi-Fi, and a lightbox was entered into HOMER Legacy tool. The software was used to

determine the best combination of the conventional grid, solar panels and wind turbines. Among all of the possible combinations, the grid connected system resulted in the lowest net present cost. It was concluded that the size of the project is too small to apply wind and solar technologies.

Thermal properties of underground soil layers in Astana were found by comparing geo-engineering report for Astana with information given in ASHRAE HVAC Handbook. After that, thermal analysis was carried out to find the underground temperature distribution in Astana. This enabled us to properly design the geothermal unit, which resulted in a horizontal geothermal system with 70m of pipes buried at 10m depth. This configuration will sufficiently serve the heat demand of the bus shelter. The construction of the new bus shelter can be completed in 31 days. It results in total cost of $11520 which is over $18000 less expensive than the current bus shelter design. Moreover, the proposed bus shelter design results in energy savings of $6159 in the course of 25 years and annual reduction of GHG emission of 2.8 tons of carbon dioxide. Finally, the extended area of the shelter can accommodate 25 more people than the current bus station. Therefore, it can be concluded that the proposed bus shelter design is more efficient, environmentally friendly, spacious and economically attractive.

## 6. References


ASHRAE Handbook "HVAC applications." *ASHRAE Handbook, Fundamentals* 2011.

ASTRA (Astana Transportation Authority). 2016. “Activity”, Available from: http://www.alrt.kz/en/activities

Bhatia, A. n.d. Heat Loss Calculations and Principles. Counting Educations and Development, Inc.

Bienfait, Dominique, Fitzner, Klaus, Lindvall, Thomas Seppanen, Folli, Woolliscroft, Michael, Fanger, P. Ole , Jantunen, Malti, Skaret, Eimund and Schwer, Joseph. 1992. *Guidelines for Ventilation Requirements in Buildings.* Commission of the European Communities Directorate General for Science, Research and Development Joint Research Centre - Environment Institute.

Burdick, Arlan. 2011. Strategy Guideline: *Accurate Heating and Cooling Load Calculations.* US Department of Energy: Building Technologies Program.

Canadian GeoExchange Coalition. 2009. A Buyer’s Guide for Residential Ground Source Heat Pump Systems. Canadian GeoExchange Coalition.

CAT Information Service. How much will a heat pump cost? | CAT Information [Online]. [Cited 3 November 2016]. Available from: https://info.cat.org.uk/questions/heatpumps/how-much-will-heat-pump-cost/

Chiasson D. Andrew. 2016. Geothermal Heat Pump and Heat Engine Systems: Theory And Practice. ASME Press.

Energy Saving Trust. Energy Efficiency Best Practice in Housing. March 2004.

EPIA. 2012. “Solar Power Electricity Empowering the World”, Available from: htttp://www.epia.org/

Erdinc O. and M. Uzunoglu 2012. Optimum design of hybrid renewable systems: Overview of different approaches. *Renewable and Sustainable Energy Reviews.* pp 1412-1425.

European Geothermal Energy Council. 2009. Geothermal Heat Pumps. European Geothermal Energy Council

EWEA (The European Wind Energy Association). 2015. “Wind in power: 2015 European Statistics”

EXPO-2017 ASTANA. 2016. “Definition”, Available from: https://expo2017astana.com/en/

Ezez. 2016. "Тарифы - АСТАНАЭНЕРГОСБЫТ". Astanaenergosbyt.kz. http://www.astanaenergosbyt.kz/tarif.

Huang, Rui, Low, Steven H., Topcu, Ufuk and Chandy, K. Mani. 2011. “Optimal Design of Hybrid Energy System with PV/ Wind Turbine/ Storage: A Case Study.” Computing Mathematical Sciences, California Institute of Technology.

IEA (International Energy Association). 2014. “2014 Key World Energy Statistics”, pp. 6-28

Indexmundi. 2016."Kazakhstan - Total greenhouse gas emissions (kt of CO2 equivalent)". Indexmundi.com. Available from: http://www.indexmundi.com/facts/kazakhstan/indicator/EN.ATM.GHGT.KT.CE.

Kazmaganbetova, Meruyert; Kaishubayeva, Nazira & Mukhanov, Nurzhan. 2015. "MODELING AND OPTIMIZATION OF ENERGETIC SYSTEM IN A HYBRID SMART HOUSE". Undergraduate, Nazarbayev University.

Kavanaugh, S.P., K. Rafferty. 1997. *Ground-Source Heat Pumps: Design of Geothermal Systems for Commercial and Institutional Buildings*, Chapter 3. Atlanta: ASHRAE

Meyer, Jason, Pride, Dominique, O’Toole, Jonathan, Craven, Colin and Spencer, Vanessa. 2011. *Ground Source Heat Pumps in Cold Climates*. Alaska Center for Energy and Power and Cold Climate Housing Research Center for Denali Commission.

Mohammed, Omar Hazem, Amirat, Yassine, Feld, Gilles and Benbouzid, Mohamed. 2016. “Hybrid Generation Systems Planning Expansion Forecast State of the Art Review: Optimal Design vs Technical and Economical Constraints.” *Journal Electrical Systems* 12(1): 20-32

Natural Resources. Canada. RETScreen [Online]. September 2016 [cited 19 November 2016]. Available from: http://www.nrcan.gc.ca/energy/software-toos/7465

Ospanova G. E, 2012. “Скважина 561-12”

Pennsylvania Clean Streams Law. 2000. “Ground source heat pumps.” Commonwealth of Pennsylvania Department of environmental protection bureau of water supply management. Volume 26, Tab 01D

Philippe, Mikael, Bernier, Michel, and Marchio, Dominique. 2010. Vertical Geothermal Borefields. *ASHRAE Journal.* www.ashrae.org

«Plast Invest Production». 2017. Водяные трубы из полиэтилена HDPE 100. Available from: http://www.plastinvest.kz/public/price-lists/2016/05/ru/voda_truby_ru_2016_PlastInvest_Production.pdf

PVInsights. 2011. “PVInsights announces worldwide 2010 top 10 ranking of PV module makers”, Available from: htttp://www.pvinsights.com/

Rawlings, Rosemary, Parker , John, Breembroek, Gerdi, Cherruault, Jean-Yves, Curtis, Robin, Freeborn, Richard, Moore, Phil, Sinclair, John, Wood, Raymond and Sandstrom, Bengt. 2004. *Domestic Ground Source Heat Pumps: Design and installation of closed-loop systems.* BRE’s Sustainable Energy Centre.

RETScreen. 2015. Windows. Varennes: Natural Resources Canada.

Rfc.Kegoc. 2016. "В КАЗАХСТАНЕ УТВЕРЖДЕНЫ ТАРИФЫ НА «ЗЕЛЕНУЮ» ЭЛЕКТРОЭНЕРГИЮ | ТОО "Расчетно-финансовый центр по поддержке возобновляемых источников энергии"". АО «KEGOC». http://www.rfc.kegoc.kz/v-kazaxstane-utverzhdeny-tarify-na-zelenuyu-elektroenergiyu/.

Smil, Vaclav 1991, *"General Energetics Energy in the Biosphere and Civilization"*, John Wiley, New York, p. 240

Solar Power Europe. 2012. "Global Market Outlook for Photovoltaics until 2016", pp. 9-64

The Eco Experts. 2016"Compare Solar Panel Prices in Your Area." | Find Installers & Compare UK Prices. January 15, 2016. Accessed November 15, 2016. Available from: http://www.theecoexperts.co.uk/.

Tiernan, Maury. 1997. "The People Load". *Commercial Modular Construction Magazine.* Geary Pacific Coorporation.

Time and Date. 2016. Available from: https://www.timeanddate.com/worldclock/kazakstan/astana

Trading Economics. 2016. Kazakhstan Inflation Rate Forecast 2016-2020. Available from: http://www.tradingeconomics.com/kazakhstan/inflation-cpi/forecast

UNDP/GEF and Government of Kazakhstan. 2006. "Report: Prospective of Wind Power Development in Kazakhstan", pp. 1-15

UNDP Kazakhstan. 2009. "Astana Wind Farm: Pre-feasibility study", UNDP Kazakhstan Wind Power Market Development Initiative, pp. 1-18

US Department of Energy. 2011. *Guide to Geothermal Heat Pumps.* US Department of Energy.

WWEA (The World Wind Energy Association). 2014. "2014 Half-year Report", pp. 1-8

Xing Lu, 2014, "Estimations of Undistributed Ground Temperatures Using Numerical and Analytical Modeling", Oklahoma State University

"АО «ПАВЛОДАРЭНЕРГО»." Тарифы. April 2017. Accessed April 10, 2017. http://pavlodarenergo.kz/ru/pavlodarenergosbyt/tarifs.html.

"Буровые/Земляные работы." Логотип Пульс Цен.ру. N.p., 13 Nov. 2016. Web. 10 Mar. 2017.http://astana.pulscen.kz/products/bureniye_skvazhin_na_vodu_31199084, http://astana.pulscen.kz/price/180801-zemljanye-raboty/f:31188_ghidromiekhanichieski

## 7. Appendices

## Appendix A

Table A.1. Ground Source Heat Pump (GSHP) system components (Adopted from Alaska center for energy and power, (Meyer, 2011).

| Main component | Sub component | Description |
|---|---|---|
| Ground loop | Tubing | Commonly a high-density polyethylene pipe, acts as a heat exchanger in the ground or water body. |
| | Working fluid | Water is mixed with either ethylene glycol, methyl alcohol, potassium acetate or other substances to lower the freezing temperature. This is the medium that transfers energy from the source to the heat pump. Open loop systems, especially in warmer climates, can use ground water directly. |
| | Pump | A circulating pump is used to move the working fluid through the ground loop and heat exchanger. |
| | Manifold | A plumbing connection where individual tubing loops are combined. This is useful in combination with valves to isolate loops. |
| Heat pump unit | Evaporator | The heat exchanger where working fluid from the ground loop passes its heat to the liquid refrigerant in the heat pump loop, evaporating it into a gas. |
| | Compressor | The compressor draws the refrigerant from the evaporator then compresses it. Compression adds energy to the refrigerant by raising the pressure and temperature to a desired level. |
| | Condenser | Heat exchange extracts the energy from the hot refrigerant to be used for heating, condensing the refrigerant gas back into a liquid. |
| | Expansion valve | This valve reduces the pressure and temperature of the refrigerant, returning it to its original state. |
| | Controls | Typically, the heat pump operation is centrally controlled and takes into account the ground-loop flow rate and room temperatures, among other variables. |
| | Desuperheater (optional) | This device extracts heat during the refrigerant cycle to produce domestic hot water (DWH). |
| Heat distribution | Hydronic | Fluid heated from the heat pump is circulated through a series of tubes embedded in flooring or panels and radiates the heat. |
| | Forced air | Air from the heat pump passes through ducts to rooms requiring heat. |

## Appendix B

Table B1. Total heat load calculation

| Month | Period of time | 6 am - 8 am | 8 am - 10 am | 10 am - 12 pm | 12 pm - 2 pm | 2 pm - 4 pm | 4 pm - 6 pm | 6 pm - 8 pm | 8 pm - 10 pm | 10 pm - 12 am |
|---|---|---|---|---|---|---|---|---|---|---|
| January | ***Average No of people*** | ***36*** | ***10*** | | ***25*** | ***15*** | | ***50*** | ***12*** | |
| | Amount of heat delievered by people in kW | 4.219 | 1.172 | | 2.931 | 1.758 | | 5.862 | 1.407 | |
| | Total heat load with no people in space in kW | 8.322 | 5.730 | | 7.226 | 6.229 | | 9.718 | 5.929 | |
| | Total heat load with people in space in kW | 4.103 | 4.558 | | 4.295 | 4.471 | | 3.856 | 4.522 | |
| February | ***Average No of people*** | ***36*** | ***10*** | | ***25*** | ***15*** | | ***50*** | ***12*** | |
| | Amount of heat delievered by people in kW | 4.219 | 1.172 | | 2.931 | 1.758 | | 5.862 | 1.407 | |
| | Total heat load with no people in space in kW | 8.335 | 5.743 | | 7.239 | 6.242 | | 9.731 | 5.942 | |
| | Total heat load with people in space in kW | 4.116 | **4.571** | | 4.308 | 4.484 | | 3.869 | 4.535 | |
| March | ***Average No of people*** | ***36*** | ***10*** | | ***25*** | ***15*** | | ***50*** | ***12*** | |
| | Amount of heat delievered by people in kW | 4.219 | 1.172 | | 2.931 | 1.758 | | 5.862 | 1.407 | |
| | Total heat load with no people in space in kW | 6.586 | 4.513 | | 5.709 | 4.911 | | 7.703 | 4.911 | |
| | Total heat load with people in space in kW | 2.367 | 3.341 | | 2.778 | 3.153 | | 1.841 | 3.504 | |
| April | ***Average No of people*** | ***36*** | ***10*** | | ***25*** | ***15*** | | ***50*** | ***12*** | |
| | Amount of heat delievered by people in kW | 4.219 | 1.172 | | 2.931 | 1.758 | | 5.862 | 1.407 | |
| | Total heat load with no people in space in kW | 3.637 | 2.452 | | 3.135 | 2.680 | | 4.275 | 2.543 | |
| | Total heat load with people in space in kW | -0.582 | 1.280 | | 0.204 | 0.922 | | -1.587 | 1.136 | |
| May | ***Average No of people*** | ***36*** | ***10*** | | ***25*** | ***15*** | | ***50*** | ***12*** | |
| | Amount of heat delievered by people in kW | 4.219 | 1.172 | | 2.931 | 1.758 | | 5.862 | 1.407 | |
| | Total heat load with no people in space in kW | 1.630 | 1.111 | | 1.411 | 1.211 | | 1.909 | 1.151 | |
| | Total heat load with people in space in kW | -2.589 | -0.061 | | -1.520 | -0.547 | | -3.953 | -0.256 | |
| June | ***Average No of people*** | ***36*** | ***10*** | | ***25*** | ***15*** | | ***50*** | ***12*** | |
| | Amount of heat delievered by people in kW | 4.219 | 1.172 | | 2.931 | 1.758 | | 5.862 | 1.407 | |
| | Total heat load with no people in space in kW | 0.235 | 0.160 | | 0.203 | 0.175 | | 0.274 | 0.166 | |
| | Total heat load with people in space in kW | -3.984 | -1.012 | | -2.728 | -1.583 | | -5.588 | -1.241 | |

| Month | Period of time | 6 am - 8 am | 8 am - 10 am | 10 am - 12 pm | 12 pm - 2 pm | 2 pm - 4 pm | 4 pm - 6 pm | 6 pm - 8 pm | 8 pm - 10 pm | 10 pm - 12 am |
|---|---|---|---|---|---|---|---|---|---|---|
| July | ***Average No of people*** | ***36*** | ***10*** | | ***25*** | ***15*** | | ***50*** | ***12*** | |
| | Amount of heat delievered by people in kW | 4.219 | 1.172 | | 2.931 | 1.758 | | 5.862 | 1.407 | |
| | Total heat load with no people in space in kW | -0.275 | -0.200 | | -0.243 | -0.215 | | -0.314 | -0.206 | |
| | Total heat load with people in space in kW | -4.494 | -1.372 | | -3.174 | -1.973 | | -6.176 | -1.613 | |
| August | ***Average No of people*** | ***36*** | ***10*** | | ***25*** | ***15*** | | ***50*** | ***12*** | |
| | Amount of heat delievered by people in kW | 4.219 | 1.172 | | 2.931 | 1.758 | | 5.862 | 1.407 | |
| | [illegible] no people in space in kW | 0.612 | 0.389 | | 0.518 | 0.432 | | 0.731 | 0.407 | |
| | Total heat load with people in space in kW | -3.607 | -0.783 | | -2.413 | -2.499 | | -5.131 | -1 | |
| September | ***Average No of people*** | ***36*** | ***10*** | | ***25*** | ***15*** | | ***50*** | ***12*** | |
| | Amount of heat delievered by people in kW | 4.219 | 1.172 | | 2.931 | 1.758 | | 5.862 | 1.407 | |
| | Total heat load with no people in space in kW | 1.935 | 1.302 | | 1.667 | 1.424 | | 2.277 | 1.350 | |
| | Total heat load with people in space in kW | -2.284 | 0.13 | | -1.264 | -0.334 | | -3.585 | -0.057 | |
| October | ***Average No of people*** | ***36*** | ***10*** | | ***25*** | ***15*** | | ***50*** | ***12*** | |
| | Amount of heat delievered by people in kW | 4.219 | 1.172 | | 2.931 | 1.758 | | 5.862 | 1.407 | |
| | Total heat load with no people in space in kW | 4.120 | 2.787 | | 3.556 | 3.043 | | 4.838 | 2.889 | |
| | Total heat load with people in space in kW | -0.099 | 1.615 | | 0.625 | 1.285 | | -1.024 | 1.482 | |
| November | ***Average No of people*** | ***36*** | ***10*** | | ***25*** | ***15*** | | ***50*** | ***12*** | |
| | Amount of heat delievered by people in kW | 4.219 | 1.172 | | 2.931 | 1.758 | | 5.862 | 1.407 | |
| | Total heat load with no people in space in kW | 5.988 | 4.136 | | 5.204 | 4.492 | | 6.985 | 4.279 | |
| | Total heat load with people in space in kW | 1.769 | 2.964 | | 2.273 | 2.734 | | 1.123 | 2.872 | |
| December | ***Average No of people*** | ***36*** | ***10*** | | ***25*** | ***15*** | | ***50*** | ***12*** | |
| | Amount of heat delievered by people in kW | 4.219 | 1.172 | | 2.931 | 1.758 | | 5.862 | 1.407 | |
| | Total heat load with no people in space in kW | 7.592 | 5.282 | | 6.589 | 5.677 | | 8.868 | 5.404 | |
| | Total heat load with people in space in kW | 3.373 | 4.110 | | 3.658 | 3.909 | | 3.006 | 3.997 | |

Table B2. Calculated electric loads by hours and months

| January | 6 am - 8 am | 8 am - 10 am | 10 am - 12 pm | 12 pm - 2 pm | 2 pm - 4 pm | 4 pm - 6 pm | 6 pm - 8 pm | 8 pm - 10 pm | 10 pm - 12 am |
|---|---|---|---|---|---|---|---|---|---|
| | **36** | **10** | | **25** | **15** | | **50** | **12** | |
| Geothermal | 0.571 | 0.571 | | 0.571 | 0.571 | | 0.571 | 0.571 | |
| Heater | 2.103 | 2.558 | | 2.295 | 2.471 | | 1.856 | 2.522 | |
| Total | 2.946 | 3.401 | | 3.138 | 3.314 | | 2.699 | 3.365 | |

| February | 6 am - 8 am | 8 am - 10 am | 10 am - 12 pm | 12 pm - 2 pm | 2 pm - 4 pm | 4 pm - 6 pm | 6 pm - 8 pm | 8 pm - 10 pm | 10 pm - 12 am |
|---|---|---|---|---|---|---|---|---|---|
| | **36** | **10** | | **25** | **15** | | **50** | **12** | |
| Geothermal | 0.571 | 0.571 | | 0.571 | 0.571 | | 0.571 | 0.571 | |
| Heater | 2.116 | 2.571 | | 2.308 | 2.484 | | 1.869 | 2.535 | |
| Total | 2.959 | 3.414 | | 3.151 | 3.327 | | 2.712 | 3.378 | |

| March | 6 am - 8 am | 8 am - 10 am | 10 am - 12 pm | 12 pm - 2 pm | 2 pm - 4 pm | 4 pm - 6 pm | 6 pm - 8 pm | 8 pm - 10 pm | 10 pm - 12 am |
|---|---|---|---|---|---|---|---|---|---|
| | **36** | **10** | | **25** | **15** | | **50** | **12** | |
| Geothermal | 0.571 | 0.571 | | 0.571 | 0.571 | | 0.526 | 0.571 | |
| Heater | 0.367 | 1.341 | | 0.778 | 1.153 | | 0 | 1.504 | |
| Total | 1.210 | 2.184 | | 1.621 | 1.996 | | 0.798 | 2.347 | |

| April | 6 am - 8 am | 8 am - 10 am | 10 am - 12 pm | 12 pm - 2 pm | 2 pm - 4 pm | 4 pm - 6 pm | 6 pm - 8 pm | 8 pm - 10 pm | 10 pm - 12 am |
|---|---|---|---|---|---|---|---|---|---|
| | **36** | **10** | | **25** | **15** | | **50** | **12** | |
| Geothermal | 0.166 | 0.365 | | 0.058 | 0.263 | | 0.453 | 0.324 | |
| Heater | 0 | 0 | | 0 | 0 | | 0 | 0 | |
| Total | 0.438 | 0.637 | | 0.330 | 0.535 | | 0.725 | 0.596 | |

| May | 6 am - 8 am | 8 am - 10 am | 10 am - 12 pm | 12 pm - 2 pm | 2 pm - 4 pm | 4 pm - 6 pm | 6 pm - 8 pm | 8 pm - 10 pm | 10 pm - 12 am |
|---|---|---|---|---|---|---|---|---|---|
| | **36** | **10** | | **25** | **15** | | **50** | **12** | |
| Geothermal | 0.571 | 0.017 | | 0.434 | 0.156 | | 0.571 | 0.073 | |
| Heater | 0 | 0 | | 0 | 0 | | 0 | 0 | |
| Total | 0.843 | 0.289 | | 0.706 | 0.428 | | 0.843 | 0.345 | |

| June | 6 am - 8 am | 8 am - 10 am | 10 am - 12 pm | 12 pm - 2 pm | 2 pm - 4 pm | 4 pm - 6 pm | 6 pm - 8 pm | 8 pm - 10 pm | 10 pm - 12 am |
|---|---|---|---|---|---|---|---|---|---|
| | **36** | **10** | | **25** | **15** | | **50** | **12** | |
| Geothermal | 0.571 | 0.289 | | 0.571 | 0.452 | | 0.571 | 0.354 | |
| Heater | 0 | 0 | | 0 | 0 | | 0 | 0 | |
| Total | 0.843 | 0.561 | | 0.843 | 0.724 | | 0.843 | 0.626 | |

| July | 6 am - 8 am | 8 am - 10 am | 10 am - 12 pm | 12 pm - 2 pm | 2 pm - 4 pm | 4 pm - 6 pm | 6 pm - 8 pm | 8 pm - 10 pm | 10 pm - 12 am |
|---|---|---|---|---|---|---|---|---|---|
| | **36** | **10** | | **25** | **15** | | **50** | **12** | |
| Geothermal | 0.571 | 0.392 | | 0.571 | 0.563 | | 0.571 | 0.461 | |
| Heater | 0 | 0 | | 0 | 0 | | 0 | 0 | |
| Total | 0.843 | 0.664 | | 0.843 | 0.835 | | 0.843 | 0.732 | |

| August | 6 am - 8 am | 8 am - 10 am | 10 am - 12 pm | 12 pm - 2 pm | 2 pm - 4 pm | 4 pm - 6 pm | 6 pm - 8 pm | 8 pm - 10 pm | 10 pm - 12 am |
|---|---|---|---|---|---|---|---|---|---|
| | **36** | **10** | | **25** | **15** | | **50** | **12** | |
| Geothermal | 0.571 | 0.223 | | 0.571 | 0.571 | | 0.571 | 0.286 | |
| Heater | 0 | 0 | | 0 | 0 | | 0 | 0 | |
| Total | 0.843 | 0.495 | | 0.843 | 0.843 | | 0.843 | 0.557 | |

| September | 6 am - 8 am | 8 am - 10 am | 10 am - 12 pm | 12 pm - 2 pm | 2 pm - 4 pm | 4 pm - 6 pm | 6 pm - 8 pm | 8 pm - 10 pm | 10 pm - 12 am |
|---|---|---|---|---|---|---|---|---|---|
| | **36** | **10** | | **25** | **15** | | **50** | **12** | |
| Geothermal | 0.571 | 0.0371 | | 0.571 | 0.095 | | 0.571 | 0.016 | |
| Heater | 0 | 0 | | 0 | 0 | | 0 | 0 | |
| Total | 0.843 | 0.309 | | 0.843 | 0.367 | | 0.843 | 0.288 | |

| October | 6 am - 8 am | 8 am - 10 am | 10 am - 12 pm | 12 pm - 2 pm | 2 pm - 4 pm | 4 pm - 6 pm | 6 pm - 8 pm | 8 pm - 10 pm | 10 pm - 12 am |
|---|---|---|---|---|---|---|---|---|---|
| | **36** | **10** | | **25** | **15** | | **50** | **12** | |
| Geothermal | 0.028 | 0.461 | | 0.178 | 0.367 | | 0.292 | 0.423 | |
| Heater | 0 | 0 | | 0 | 0 | | 0 | 0 | |
| Total | 0.300 | 0.733 | | 0.450 | 0.639 | | 0.564 | 0.695 | |

| November | 6 am - 8 am | 8 am - 10 am | 10 am - 12 pm | 12 pm - 2 pm | 2 pm - 4 pm | 4 pm - 6 pm | 6 pm - 8 pm | 8 pm - 10 pm | 10 pm - 12 am |
|---|---|---|---|---|---|---|---|---|---|
| | **36** | **10** | | **25** | **15** | | **50** | **12** | |
| Geothermal | 0.505 | 0.571 | | 0.571 | 0.571 | | 0.320 | 0.571 | |
| Heater | 0 | 0.964 | | 0.273 | 0.734 | | 0 | 0.872 | |
| Total | 0.777 | 1.807 | | 1.116 | 1.577 | | 0.592 | 1.715 | |

| December | 6 am - 8 am | 8 am - 10 am | 10 am - 12 pm | 12 pm - 2 pm | 2 pm - 4 pm | 4 pm - 6 pm | 6 pm - 8 pm | 8 pm - 10 pm | 10 pm - 12 am |
|---|---|---|---|---|---|---|---|---|---|
| | **36** | **10** | | **25** | **15** | | **50** | **12** | |
| Geothermal | 0.571 | 0.571 | | 0.571 | 0.571 | | 0.571 | 0.571 | |
| Heater | 1.373 | 2.11 | | 1.658 | 1.909 | | 1.006 | 1.997 | |
| Total | 2.216 | 2.953 | | 2.501 | 2.752 | | 1.849 | 2.840 | |

## Appendix C

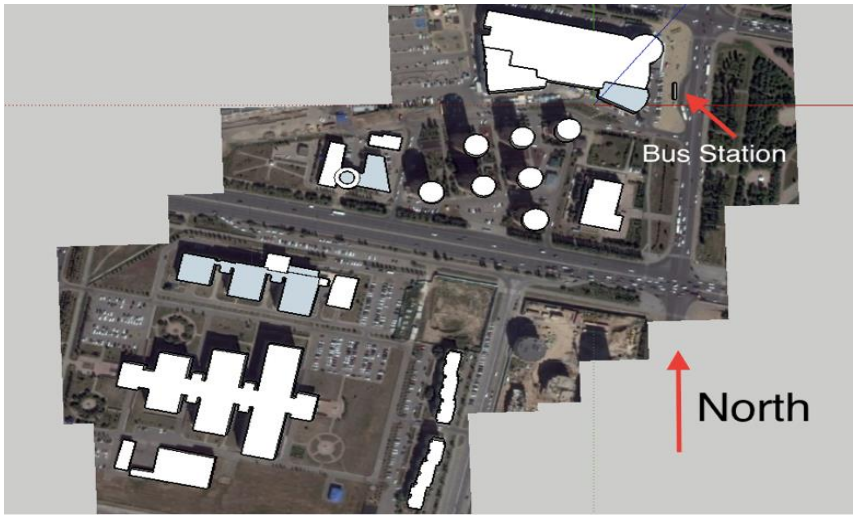


Figure C.1. Top view of CAD model

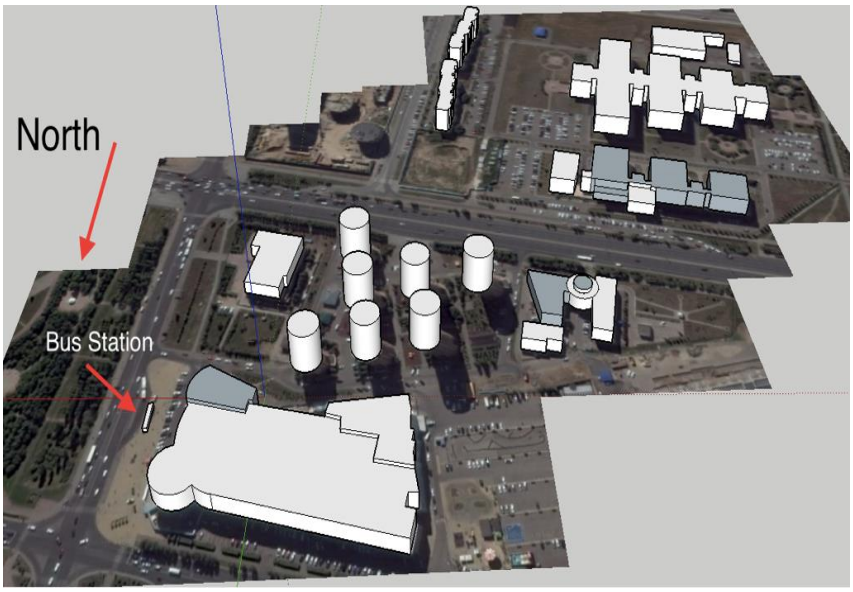


Figure C.2. Side view of CAD model

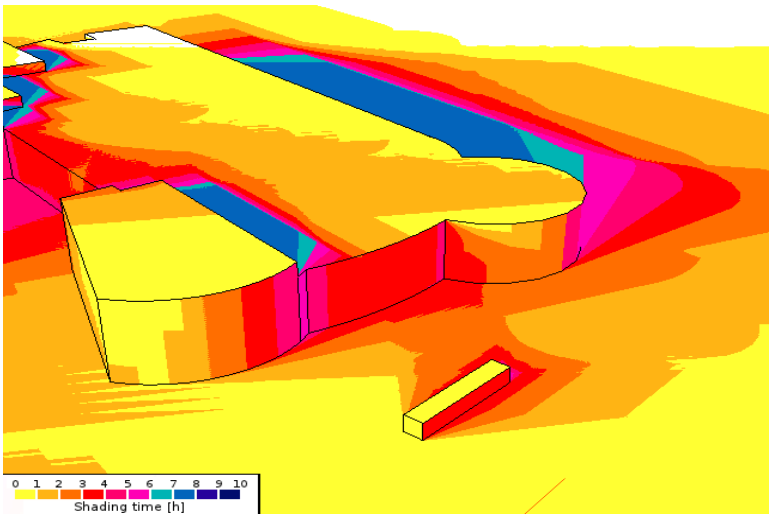


Figure C.3. Shadow Analysis simulation result for December 21.

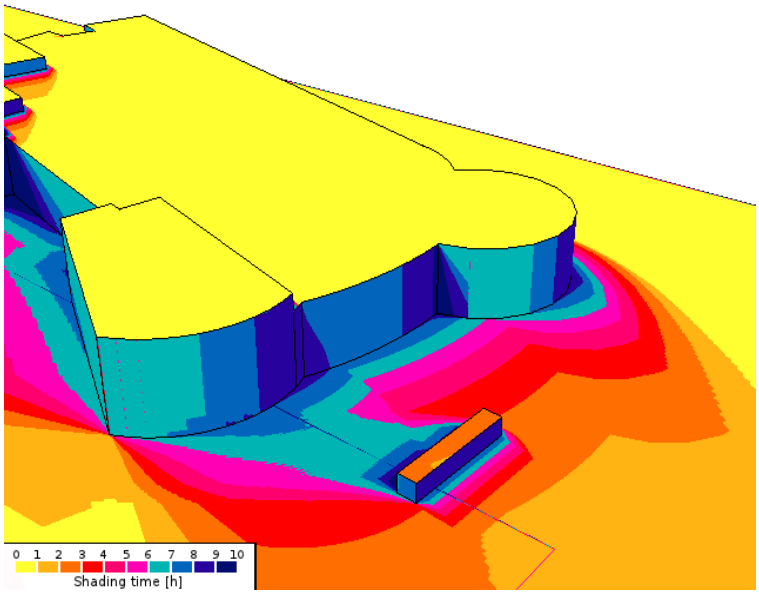


Figure C.4. Shadow Analysis simulation result for June 21

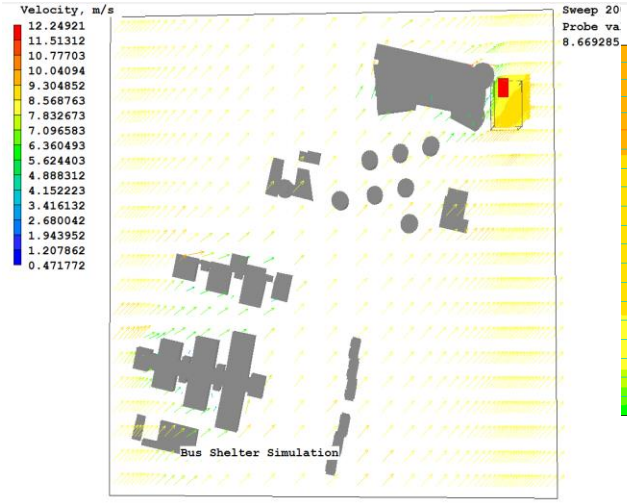


Figure C.5. Top view of the simulation results for January

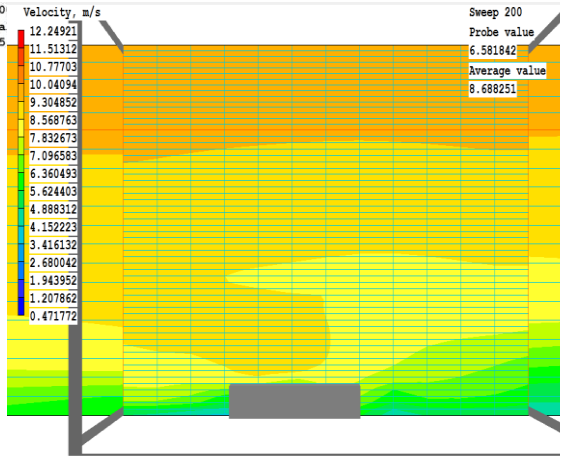


Figure C.6. East view of the simulation results for January

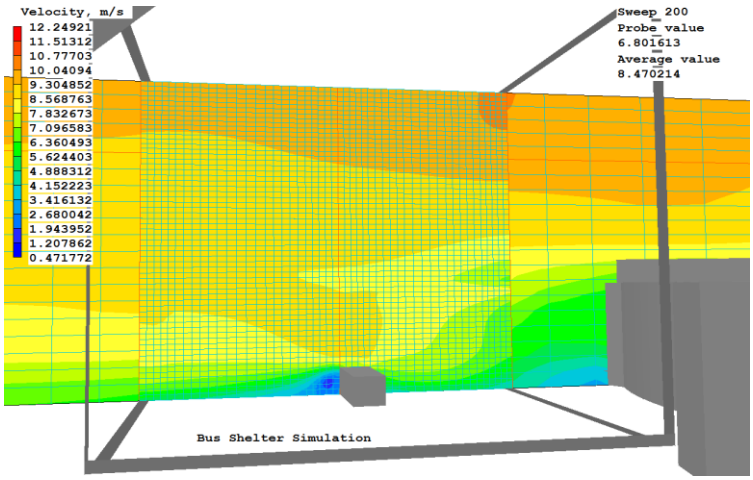


Figure C.7. North view of the simulation results for January

## Appendix D

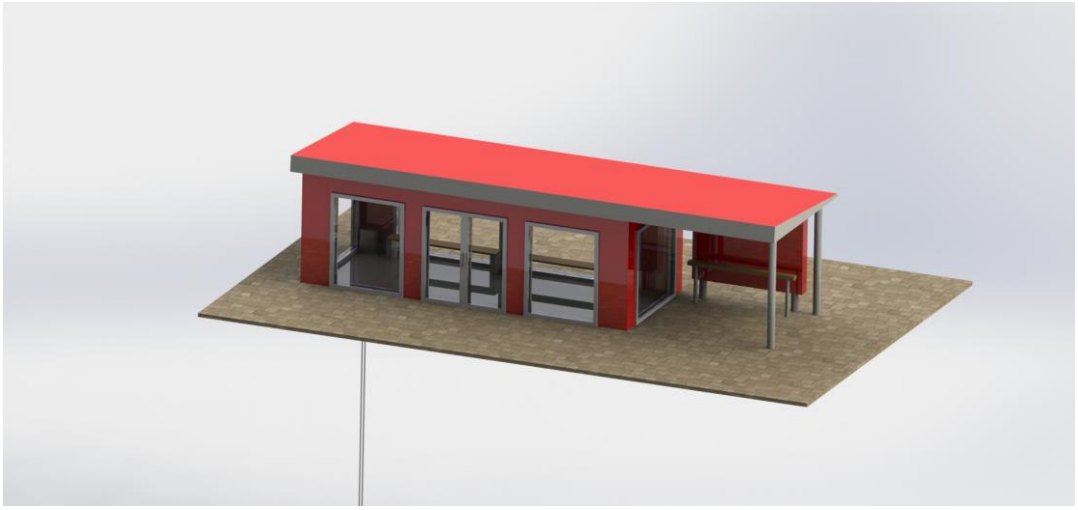

Figure D.1. 3D CAD Model of proposed shelter: view 1

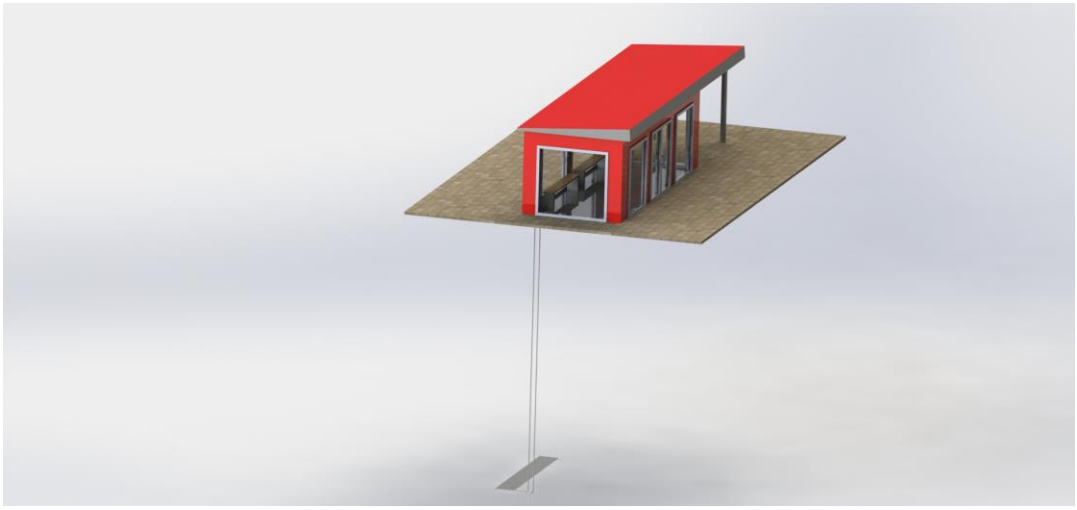

Figure D.2. 3D CAD Model of proposed shelter: view 2

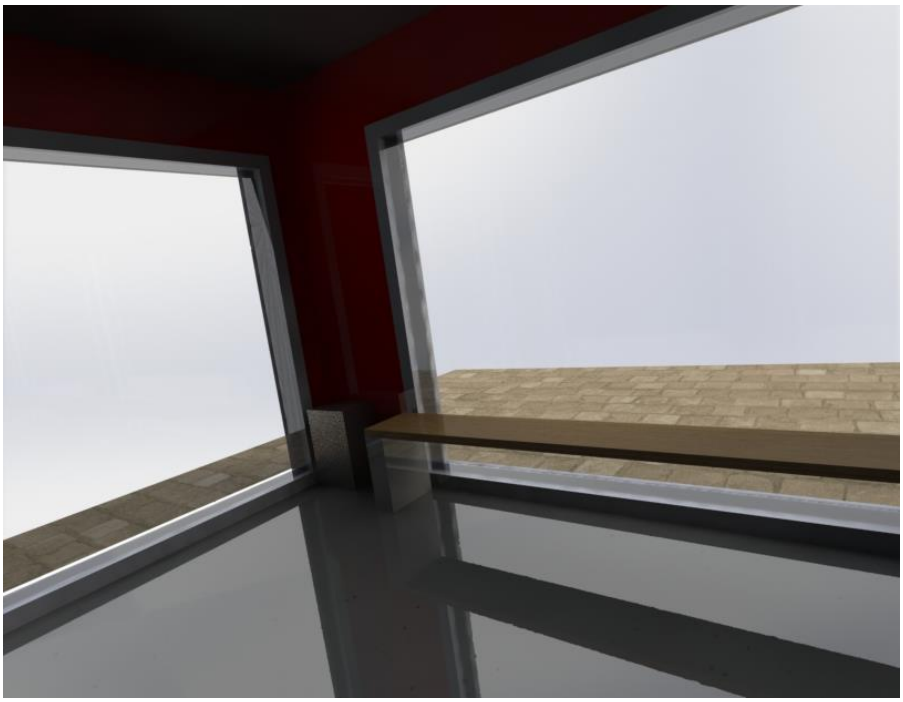

Figure D.3. 3D CAD Model of proposed shelter: interior view 1

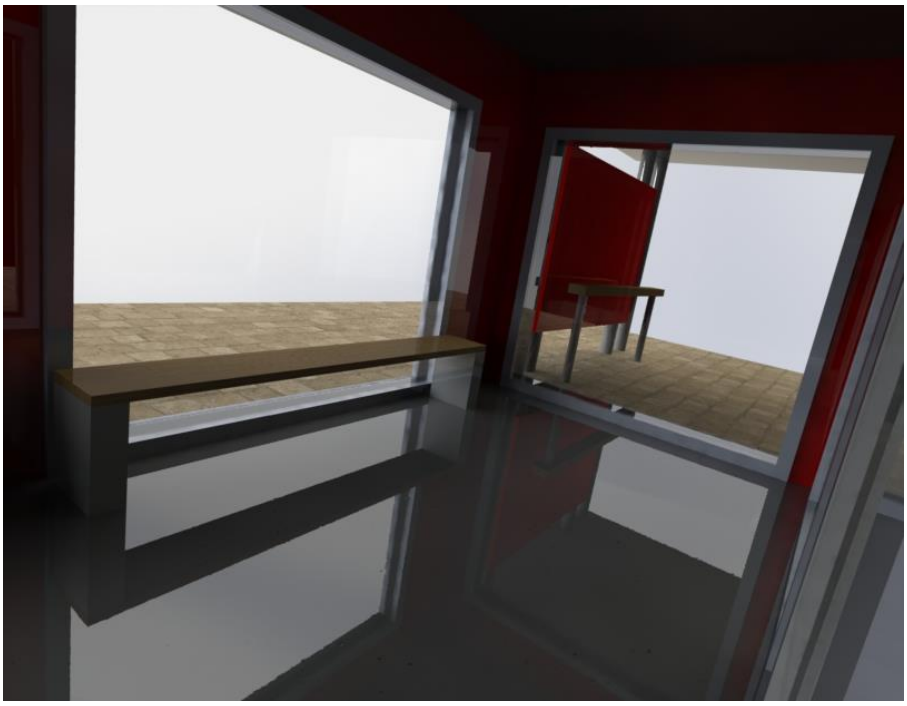

Figure D.4. 3D CAD Model of proposed shelter: interior view 2